A U B U R N U N I V E R S I T Y

SCHOOL OF ENGINEERING
Department of Mechanical Engineering

Report No. II

PRELIMINARY INVESTIGATION OF PRESSURE INFLUENCE ON MULTIPHASE HEAT TRANSFER

R. I. Vachon
G. E. Tanger
R. B. Pollard
D. L. Davis

under contract with
NATIONAL AERONAUTICS AND SPACE ADMINISTRATION
GEORGE C. MARSHALL SPACE FLIGHT CENTER
Contract No. NAS8-11234

November, 1964

ABSTRACT

The literature on the effect of transient pressure on nucleate-boiling has been surveyed. The interrelation of boiling parameters with pressure is discussed. The discussion is based on the assumption that a transient pressure boiling process is an infinite number of steady-state processes (quasi-static).

The methods of describing surface texture are discussed. A review of the mechanism of ebullition in boiling heat transfer indicates the necessity of adequate nucleation sites. Corrosion as a means of providing the nucleation sites is discussed.

Author

TABLE OF CONTENTS

LIST OF FIGURES

LIST OF TABLES

NOMENCLATURE

A. Letter Symbols

Symbol		Dimensional Units
A	Area	ft^2
b	Pit depth	in.
C_5	Constant in Exponent of eq. (19)	
C_L	Heat Capacity of liquid	Btu/lb_m
D_o	Bubble breakoff diameter	in.
D	Diameter of cavity	in.
d	Pit diameter	in.
f	Bubble frequency	sec^{-1}
g	Acceleration due to gravity	ft/sec^2
go	Gravitational constant	$lb_m\ ft/lb_f\ sec^2$
h_{f_g}	Latent heat of vaporization	Btu/lb_m
h	Convective heat-transfer coefficient	$Btu/hr\ ft^2\ °F$
J	Joule's equivalent	$ft\text{-}lb_f/Btu$
K	Constant in eqs. (5) and (19)	
k	Thermal conductivity	$Btu/hr\ ft\ °F$
L	Length over which average is taken	
M	Molecular weight	$lb_m\text{-}mole/lb_m$
m	Exponent in eqs. (1) and (5)	
n	Number of active sites	
P	Pressure	lb_f/in^2
Q	Heat flow rate	Btu/hr
q	Heat flux	$Btu/hr\ ft^2$

Symbol		Dimensional Units
r	Cavity radius	in.
R	Specific gas constant	ft-lb_f/lb_m °R
$\mathcal{R}$	Universal gas constant	ft-lb_f/lb_m-mole °F
T	Temperature	°F
t	Time	sec
V	Specific volume	ft^3/lb_m
x	Distance along surface	in.
$\overline{Y}$	Root mean square average	
y	Ordinate for profile curve	

B. Greek Letters

δ	Thermal boundary layer thickenss	in.
Δ	Denotes difference in quantity that follows the symbol	
μ	Viscosity	lb_m/ft hr
ϕ	Conical angle of cavity	dimensionless, deg
ρ	Density	lb_m/ft^3
σ	Surface tension	lb_f/ft
θ	Contact angle	dimensionless, deg

C. Subscripts

L	Refers to liquid phase
max	maximum
min	minimum
s	Saturation
v	Refers to vapor phase
w	Wall

I. INTRODUCTION

Two parameters, pressure and surface condition, are of extreme importance in boiling heat transfer. These parameters have been discussed in Report I (1)*. There is a scarcity of data on pressure effects and surface conditions and a universal correlation equation does not exist for either parameter. This study is an investigation of these two parameters. The equipment for the studies has been described (1). This report discusses areas pertinent to the studies. In particular the report contains a discussion of

a) The Boiling Heat Transfer Parameter, Pressure

b) Surface Characterization

c) Surface Preparation for Surface Effects Studies

d) Data Collection

---

* Numbers in parentheses denote references cited.

II. The Boiling Heat Transfer Parameter, Pressure

A general discussion of the effect of the various boiling parameters on boiling heat transfer has been presented (1). The significance of the parameter, pressure, on boiling will be determined as a result of this study. The study will be an investigation of the effect of depressurization on boiling systems. The investigation will be restricted initially to the nucleate boiling regime where heat transfer data are usually correlated with an equation of the form

$$\frac{Q}{A} \sim \Delta T^m \tag{1}$$

Most analyses and experiments on pressure effects on boiling are for steady-state conditions. The recent bibliographies on boiling heat transfer and two-phase flow by Gouse (2) and Kepple and Tung (3) reveal an increasing interest in transient parametric effects. There are a number of studies on the effect of transients in the generated heat flux. One article on the effect of a pressure decay during nucleate pool boiling is of particular interest to this study. This work was done by Howell and Bell (4) and will be discussed along with other pertinent investigations. The effect of pulsating pressures on boiling has been investigated by Plesset and Hsieh (5) and DiCicco and Schoenhols (6). It was found that rapid pressure pulses enable a boiling system to operate safely in the film boiling regime.

The investigation by Howell and Bell was an experimental study of pressure decay on pool-boiling burnout. The range of pressures investigated by Howell and Bell was 0 to 75 psi with two different discharge rates. The discharge time was varied by insertion of an orifice plate between the boiler and release valve. Two orifice diameters, 1.5 and 3.0 inches were used. A typical pressure vs. time curve is shown in Fig. 1. The spikes in Fig. 1 are dependent to some extent on the geometry of the orifice and valve.

Before further discussion on the subject of a pressure decay or increase during boiling, a review of some of the steady-state analyses will be necessary in order to project trends during pressure transients. The review will be coupled to the assumption that a transient process is an infinite number of steady-state processes (a quasi-static process). Thus, the information from a steady-state analysis such as the effect of pressure on heat flux, liquid and wall superheat and nucleation characteristics will be considered.

As discussed in Report I (1), Griffith and Wallis (7) performed an experimental investigation on the cavity size of nucleation sites and nucleation from horizontal surfaces. A small pressure transient in the range 76 to 40 cm. of mercury was used in order to increase the liquid superheat. Liquid superheat is defined as being the difference between the liquid and saturation temperature of the test fluid. Although a transient pressure condition was investigated no information was given on the discharge time.

The effect of pressure on liquid superheat for a particular nucleation cavity size is evident from Fig. 2. As the pressure is decreased, the superheat required for the cavity to remain active has to be increased. The increasing superheat phenomena has been encountered previously by Farber and Scorah (8) and Cichelli and Bonilla (9) in their investigations on the effect of a steady-state pressure during nucleate pool boiling of water. Figures 3 and 4 show that the wall superheat increases with a decrease in pressure. Rohsenow (10) used the following equation to explain the increasing superheat.

$$T_w - T_s = \frac{R_v T_s T_v}{h_{fg}} \ln\left(1 + \frac{2\sigma}{P_L r}\right) \tag{2}$$

Equation 2 is derived by combining the Clausius-Clapeyron equation for a perfect gas and considering equilibrium at the interface of a spherical vapor bubble surrounded by a fluid. The equation describing the equilibrium is known as the Gibbs equation and for bubbles in static equilibrium is

$$P_v - P_L = \frac{2\sigma}{r} \tag{3}$$

Thus, for a bubble to grow P_v must be greater than P_L and for evaporation to occur T_L must be greater than T_v or the liquid must be superheated with respect to both itself and the vapor.

At high pressure, T_s approaches T_w and T_v is approximately equal to T_w, therefore, T_v is approximately equal to T_s. Thus, Eq. 2 can be reduced, upon expanding the log term and neglecting higher powers of pressures, to

$$T_v - T_s = \frac{2 R_v T_s^2 \sigma}{h_{fg} P_L r} \tag{4}$$

Also, it is known that particular surfaces have cavity size distributions as is shown schematically in Fig. 5 (10). It has further been verified that at a particular heat flux, a certain number of cavities must be active at different wall superheats; that is

$$\frac{Q}{A} = K \left(\frac{n}{A}\right)^m \tag{5}$$

Then given a superheat, a particular minumum size cavity, r, must be active which in turn means a certain number of nucleation sites must be active. A relation between wall superheat, critical cavity radius and nucleation sites is shown in Figs. 6 and 7. Figure 6 presented by Griffith and Wallis (7) shows how the number of active sites on a copper surface varies with wall superheat for atmospheric pressure. In Eq. 4 with r constant, we see that the superheat decreases with increasing pressure. An increased number of nucleation sites with a pressure increase causes an increase in the overall agitation effect; hence, the heat flux is increased as is evident from Eq. 5.

The experimental study of nucleate pool boiling of water at low pressures by Raben, et al., (11) revealed that not only the superheat of the surface increases as the pressure decreases, but

(a) the number of sites (n) producing bubbles at any instant decreases,

and

(b) the critical radius increases for constant superheat with decreasing pressure.

However, no smooth trend was discernible. By rearranging Eq. 4, one can see that for constant superheat, the critical site radius would

increase with a decrease in pressure. From the study of Raben, et al, and Eq. 4 one might conclude that a family of curves instead of the one shown in Fig. 6 should exist for the site density. This family of curves would depend not only on the wall superheat, but also the pressure.

Corty and Foust (12) offered an explanation for the decrease in wall superheat with increasing pressure. As the external or ambient pressure is increased the boiling point increases and the entire process of evaporation takes place at higher temperature levels. The contact angle between bubble and surface probably increases while the surface tension decreases with increasing temperature. As stated in Ref. (13) the equation

$$P_v - P_L = \frac{2\sigma}{r}\left(\cos\left(\frac{\phi}{2} - \theta\right)\right) \qquad (6)$$

must be satisfied regardless of the external pressure if the terms are adjusted for the new conditions. With increasing temperature, the righthand side of Eq. 6 will remain constant. However, the slope of the vapor pressure versus temperature curve for a liquid becomes greater with increasing pressure or temperature; thus, less wall superheat is required to provide the necessary pressure difference in Eq. 6. Figure 8 is a graph of vapor pressure versus temperature for water and illustrates the increasing slope.

The conclusion drawn by Corty and Foust is that the wall superheat required for a surface to continue boiling is decreased as the ambient or liquid pressure is increased. Therefore, the curves of Q/A versus ΔT and h versus ΔT are displaced to the left.

Kutateladze (13) performed experiments on the number of active sites promoting vapor formation for the various pressures. He derived the following equation for the site density

$$\frac{n}{A} = \frac{6}{\pi \psi} \cdot \frac{q}{h_{f_g} \rho_v D_o^3 f} \tag{7}$$

where ψ, represents the relative increase in volume of a vapor bubble from the moment it leaves the heated surface. Figure 9 is a graph of experimental data obtained by Kutateladze. As is evident from the figure, the increase in active site density is much greater than the pressure increase. The increase in active site density with pressure was explained by Kutateladze to be a result of the vapor density and vapor formation on the heated surface. The vapor density is proportional to the system pressure. Hence, the number of active sites producing vapor increases rapidly to overcome the loss in vapor generated by the heated surface with increasing pressure. The loss of vapor generation at the heated surface with increasing pressure is evident from the equation

$$\text{Rate of vapor generation} = \frac{q}{h_{f_g} \rho_v} \tag{8}$$

For constant heat flux ρ_v increases and h_{f_g} remains essentially constant as the pressure increases, hence, the rate of vapor generation at the surface decreases.

Bankoff (14) derived an equation for predicting the surface temperatures at the inception of boiling for low pressures. The equation is based on a limited real solution of equations describing the rate of penetration of a liquid into a capillary element or active site. The need to be able to predict surface temperatures for steady boiling can

be seen from Eq. 1. By predicting a single point on the line, the nucleate boiling curve for the particular conditions is then fixed. The problem was not completely solved, but an equation that approximately predicts the minimum wall superheat is

$$(T_w - T_s)_{min} = \left(\frac{X \; T \; h_{fg} \; V_L \; (V_v - V_L)}{\mu_L \; K_L \; C_L \; J} \right)^{\frac{1}{3}} \cdot \left(\frac{\sigma \cos \theta}{V_v} \right)^{\frac{2}{3}} \quad (9)$$

where $T = \frac{1}{2} (T_w + T_s)$

X = Geometric factor which is 2 for a cylindrical cavity and 4/3 for a steep wall groove.

As noted in Ref. (14), the few available pool boiling data at high pressure indicate that the critical cavity radius, r*, decreases with increasing pressure. This decrease is illustrated in Table I.

TABLE I

Variation of Critical Cavity Radius with Pressure for Water Boiling on Platinum Wire

(Data taken from Table I, Ref. 14)

Surface	Fluid	P_L lbs/in	T °F	r* cm x 10^4
0.024 in Pt wire	water	14.7	18	1.2
0.024 in Pt wire	water	383	4.4	0.3
0.024 in Pt wire	water	770	2.7	0.3
0.024 in Pt wire	water	1205	2.1	0.2
0.024 in Pt wire	water	1985	1.6	0.1

Bankoff stated that the critical cavity radius for a site to become active does not decrease with increasing pressure as was

stated by Raben, et al. (12) and shown in Table I. This conclusion was drawn from the following: (a) for a given cavity, the average rate of liquid penetration is less at higher pressures due to the increase in the volumetric heat content of the vapor and (b) the amount of heat transfer by conduction away from a cavity into the liquid is not greatly affected by pressure. The first reason given above, (a), indicates that larger cavities should become active at elevated pressures. That is, the larger cavities are not filled with a liquid at elevated pressures and hence are nucleation sites. The explanation that the larger cavities become active may explain the increase in active site density with a pressure increase. At an increased pressure, the wall superheat is less and characteristic of the least favorable active nucleus, which determines the minimum, critical cavity radius. At atmospheric pressure, a smaller bubble population is sufficient to make ebullition predominate as compared to larger bubble populations at elevated pressures, (14). Thus, an increase in the number of active sites is necessary before a change in the slope of the heat flux versus temperature-difference curve is observed.

The explanation of why the larger cavities become active may be due to a decrease in the fluid agitation near the predominant nucleation sites with an increase in pressure. The agitation is reduced due to the decrease in bubble size as pressure increases. The reduction of a agitation may reduce the sweeping action of fluid in the large cavities. This sweeping action may tend to clear the large cavities of vapor or gas before appreciable nucleation can occur. This reasoning was not

stated in Bankoff's paper but is a probable explanation. The explanation has some support from observation of a pool boiling with a pressure increase. At low or atmospheric pressure one sees a multitude of small bubbles leaving a heated surface. These bubbles are extremely small and may constitute the vapor or gas sweepings.

The effect of an elevated steady-state pressure on the active site distribution and frequency is shown in Fig. 10. The statistical nature of nucleate pool boiling is clearly indicated in the figure. The maximum number of active sites indicated by the curves in Fig. 10 designates the most probable rate of vapor bubble formation for a given set of conditions (13). As seen in the figure, the maximum number of sites decreases with an increase in pressure.

The rate of growth of vapor bubbles near a heated surface is also affected by pressure changes. Kutateladze (13) derived Eq. 10 for predicting the growth rate of bubbles on a heated surface.

$$D_o f = \frac{2q_w}{\eta\, h_{fg}\, \rho_v} \tag{10}$$

The coefficient, η, represents the time that the heated surface is in contact with the liquid from the moment a bubble leaves the surface to the moment a new bubble is generated. Kutateladze also concluded that heat flow from the liquid to a vapor bubble is not a strong function of pressure. It then follows from Eq. 10 that the rate of growth of vapor bubbles should decrease with increasing pressure. Figure 11 is a plot of the relative change of $D_o f$ with pressure. The experimental data are

accurately predicted by the equation

$$\frac{(D_o f)_P}{(D_o f)_{P=1}} = \frac{1}{P_L} \tag{11}$$

The rate of growth of vapor bubbles over the range investigated was inversely proportional to the absolute pressure. As seen from Fig. 11 this also appears to hold for aqueous solutions as well as pure water.

Earlier work on bubble growth and frequency was done by Jakob and Linke (15) and Fritz and Ende (16). In the limited range investigated, the mean bubble diameters and frequencies were found to be independent of the heat flux. Thus, the product of mean bubble diameter and frequency was considered constant for a given pressure.

$$\overline{D}_o \overline{f} = \text{const.} \tag{12}$$

A value of 77 mm/sec was obtained by (15) and 95 mm/sec by (16). The difference in the two constants appears to be due to the difference in liquid properties.

Zuber (17) also proposed an equation for predicting the mean or average bubble diameter and frequency in terms of physical properties of liquid and vapor. The equation is

$$\overline{D}_o \overline{f} = 0.59 \left(\frac{g\sigma(\rho_L - \rho_v)}{\rho_L^2} \right)^{\frac{1}{4}} \tag{13}$$

The left-hand side of Eq. 13 was found to yield 93 mm/sec and 64 mm/sec, respectively for water and carbon tetrachloride at atmospheric pressure. The cavity diameter predicted by Eq. 11 agrees closely with Jakob and Linke and Fritz and Ende. The equation, although not investigated for

various pressures should hold for pressures other than atmospheric. The pressure effect is evident in the liquid and vapor densities.

A recent investigation on saturated nucleate pool boiling by Rallis and Jawurck (18) discussed a relation given by Séméria between the minimum critical cavity radius and pressure. The equation derived by Séméria is

$$r_{min} = \frac{\text{const}}{\Delta T \; P_L} \tag{14}$$

and is applicable for water in the pressure range of 1 to 50 atm. From Eq. 14 it can be seen that at a constant superheat, the minimum critical cavity radius decreases with increasing pressure. This last statement is in conflict with the conclusion drawn earlier by Bankoff (14).

It is possible, as noted in Ref. (18), for $r_{min} = r_{max}$; that is the size range of active sites approaches zero as shown in Fig. 11. If this occurs, nucleate boiling must be expected to cease, and some other mechanism of heat transfer will evolve. This situation is possible if ΔT is decreased at some medium heat flux and low pressure. It is probable in this case that free convection would evolve as the heat-transfer mechanism. A similar but completely reversed process would probably result in film boiling.

Nucleation from solid surfaces is generated by surface cavities of different geometries. For given conditions, an active cavity size range distribution is possible, as stated in Ref. (17). The maximum size of an active cavity is determined by the thermal boundary layer above the heated surface, while the minimum size is determined by the

thermodynamics of the system. Using the assumption that the largest cavity on a surface is always active, then the thermal boundary-layer thickness, δ , must be thick enough to contain the vapor nucleus at any stage. In equation, form, this means

$$\delta \geqslant r_{max} \tag{15}$$

Equation (15) places a limit on r_{max}. The limit on r_{min} can be obtained from Eq. 4 for constant pressure and properties evaluated at the saturation temperature. Upon substitution, Eq. 4 reduces to

$$r_{min} = \frac{\text{const.}}{\Delta T} \tag{16}$$

The previous discussion on the various investigations of pressure during boiling shows the role pressure plays in nucleate boiling. As noted by Westwater, (19), some investigators believe that the only role of pressure in boiling lies in its effect on the boiling temperature and physical properties while others believe pressure to be a significant parameter. As is evident from the discussion, some conflicts exist as to how certain parameters vary with pressure. This is due in large part to the insufficient number of investigations under carefully controlled conditions.

Figure 12 shows the variation of steady-state burnout heat flux with pressure. The curve of Howell and Bell was fitted by multiple-regression analysis. The majority of all the data fell within the 95 per cent confidence limits. The test specimens used in their work were 0.0010-inch thick by 6 inches stainless steel strips, necked to 0.75 inch at the center. Burnout usually occurred during a pressure decay.

Initial pressure before a pressure release had a pronounced effect on the time required to reach burnout. A curve of Δt_s, time elapse between steady-state burnout and actual burnout, versus steady-state, initial pressure burnout heat flux is shown in Fig. 13. From the figure, it is seen that initial pressure is indeed a significant parameter in regard to the burnout point. As the initial pressure is increased the time to reach some minimum probable burnout level is decreased. The occurrence of this phenomenon might have been expected by recalling that at the higher initial pressures before release, the liquid has a higher saturation temperature, less wall superheat and a larger number of active nucleation centers (12,14). Once the pressure is released, the liquid then becomes highly superheated, more nucleating centers are activated with a greater frequency (12), resulting usually in a vapor film completely covering the surface. Once a vapor film has developed over the surface, burnout results.

If a pressure release is initiated at a low initial pressure, the time film boiling begins is delayed. The time delay is due to low liquid superheat, and very few nucleation centers. The saturation temperature does not undergo as large a change with time in a low initial pressure decay; thus the growth increase of the thermal boundary layer is reduced. The above explanation neglects any liquid agitation caused by the escaping vapor. As noted by Howell and Bell, the escaping vapor causes the liquid to be turbulent, thereby destroying the thermal boundary layer and vapor film next to the heated surface.

The nomenclature and procedure used in determining the burnout time is shown in Figs. 14 and 15. In all runs, the system in (4) was at some steady pressure and was decreased to atmospheric pressure. The heat flux as shown in Fig. 15 remains essentially constant during a pressure decay.

The effect of pressure-release rate can be seen from Fig. 16. It is interesting to note that the slower rate of release gave larger values of Δt_s regardless of the heat flux. One would expect from quasi-steady analysis that if a release rate approaching zero was chosen that Δt_s should also approach zero. That is, the process should follow the steady-state curve and point D should lie on top of point B.

In cross-plotting the data of Fig. 16 as reduced heat flux versus burnout pressure, both release rates appear to coincide, as shown in Fig. 17. Thus, it was concluded by Howell and Bell (4) that the time effect shown in Fig. 16 was due only to the rate at which burnout was approached. Figure 17 indicates, that in relation to the steady-state burnout curve, the burnout point is not displaced by the change in release rate. The conclusion drawn from comparing Figs. 16 and 17 was that over the range studied, release was probably not a significant parameter. The above explanation tends to leave the reader in doubt on the effect of release rate since a limited amount of data were presented on initial pressure.

As mentioned earlier, Howell and Bell noticed extremely rapid turbulent mixing or agitation of the test fluid in the boiler during a pressure decay, which is believed to cause the burnout heat fluxes to be higher than expected. The effect of low pressure-release rates is to decrease

the heat flux away from the test strip, while high release rates have the opposite trend. As the release rate is increased, violent agitation of the bulk fluid increases the importance of the convective heat-transfer process. These increased convective currents, along with bulk nucleation of the test fluid, tend to delay burnout past the values predicted from steady-state analysis. Although the slower transients produced equally violent agitation, burnout usually occurred at about the same pressure during the transient. However, the slower release rate made Δt_s appear larger, as shown in Fig. 16.

The conclusion drawn from (4) is for known initial pressure, heat flux, and release rate, the burnout time can be predicted provided the steady-state characteristics of the system are known. Also, pressure-release rate does not change the burnout point in relation to steady-state values. As for steady-state boiling, the peak indicated burnout temperature was always less than the melting temperature of the test strip. The time lapse of temperature excursion from the start of film boiling to burnout was approximately one second.

III. SURFACE CHARACTERIZATION

A survey of the literature on surface effect contribution to boiling heat transfer has been presented (1). This survey emphasized the difficulty in describing or characterizing surfaces employed in boiling studies. A discussion of surface characterization is presented to show the difficulties and present the method to be adopted in this study.

Most surfaces of engineering interest are extremely complex, consisting of more or less randomly distributed irregularities covering a wide range of both height and spacing. One approach to surface characterization is the representation of surface irregularities by a graph of irregularity height or depth versus surface length. A record of this type can be obtained with a tracing stylus which is moved along the surface. Optical measuring devices or techniques are another approach to the surface-characterization problem.

The quantity which has been found most useful in characterizing a surface is the average roughness height.* Consider a surface to be composed of hills and valleys, then each valley or hill has a median line which can be referred to as its center line. The arithmetical average deviation from the center line is given by:

$$Y = \frac{1}{L}\int_{x=0}^{x=L} y\, dx \qquad (17)$$

---

* "Extracted from Surface Texture (ASA B46. 1-1962), with permission of the publisher. The American Society of Mechanical Engineers, United Engineering Center, 345 East 47th Street, New York, 17, N.Y."

The unit employed in most electrical measuring instruments is the root mean square average defined by:

$$\overline{Y} = \frac{1}{L}\int_{x=0}^{x=L} y^2 dx \,^{\frac{1}{2}} \tag{18}$$

The method used in measuring this average roughness is to move a sharp-pointed stylus over the surface and translate its motion perpendicular to the surface into a meter reading proportional to the average roughness. Surface boiling data have been correlated using the Profilometer and a comparison of data obtained in this study with data of other studies must be made using similar descriptive techniques. Berenson (20) has shown the Profilometer does not represent the ultimate means of surface description.

Another instrument, the Linear Proficorder, manufactured by the Micrometrical Division of Bendix Corporation, has been used by F. G. Hammitt, et al (21) in cavitation studies at the University of Michigan. This instrument has the capability of measuring and indicating the pit depth-to-diameter ratio due to cavitation. The Linear Proficorder is being considered for this study and will be discussed below in detail. It should be mentioned that any device that makes physical contact with the surface is undesirable since the surface is altered by the stylus and it is not always possible to evaluate the alteration. The Linear Proficorder measures the diameter-to-depth ratio of the pits and scratches on the surface. The correlation of boiling heat transfer data using the diameter-to-depth ratio represents a fresh approach to the surface characterization problem. The ratio will be used as the exponent of the correlation Eq. (1) discussed previous-

ly in Chapter II. The equation has the form

$$\frac{Q}{A} = K \left(\frac{n}{A}\right)^{m} \tag{5}$$

which can be rearranged as

$$\frac{Q}{A} = K \left(\frac{n}{A}\right)^{C_5 \frac{d}{b}} \tag{19}$$

The ratio d/b may prove useful in correlating boiling heat-transfer data without going to experimental methods for untested conditions. Hammitt (21) has shown cavitation pits exhibit diameter-to-depth ratios of the same magnitude as the exponent used in correlation equations by Gaertner and Westwater (22). This may be coincidental but it appears to be one avenue for investigation. C_5 and K will be used in an attempt to adjust the equation for various pressures. Other investigators such as Jakob and Corty and Foust have found this exponent also.

Two methods, in addition to the Linear Proficorder for obtaining the diameter-to-depth ratio, are being considered. One of the most promising methods appears to be the use of optical comparators or instruments such as a Bausch & Lomb Scratch Depth Guage. The surface is not touched in the measuring process. The other method being considered is the application of a thin film of ethylene dichloride containing 1 per cent by weight of Formvar (23). When the film dries and hardens, a mesh screen can be placed in contact with the area to be tested. A circular incision can be made around the area and the replica may then be stripped from the specimen. To strengthen and facilitate handling, the replica may be coated with chromium in a vacuum furnace. This is accomplished by heating, vaporizing and

condensing the chromium on the replica. Electron and optical photo-micrographs may be taken of the replica and the topographic variations obtained. This last technique is a time-consuming process and it is not known whether this method will provide greater accuracy than the Linear Proficorder.

There are a number of ways to characterize surfaces as can be seen. A search of the boiling literature reveals that in addition to photographs and photo-micrographs of the surface some authors have attempted to define the surface by the number of active sites per unit area. This is a difficult method of description.

It appears that the sound approach to follow will involve

1) Comparison of data with previous investigators using the Profilometer.
2) Comparison of data with previous investigations using the Linear Proficorder, an optical comparator, or the shadow casting of a film replica.

IV. Surface Preparation for Surface Effects Studies

a) Discussion

The complexity of surface description is interrelated to surface preparation. One of the most desirable characteristics of any experiment is the reproducibility of data. In boiling heat transfer each experimenter who has worked with surface effects has had his own technique for surface preparation. The majority of surface effects studies have concentrated on the effect of various polished surfaces on boiling. The techniques employed for surface preparation are varied. Some authors choose to polish specimens by stroking in one direction only. Others prefer to stroke in one direction until all visible scratches are removed, then use a finer grade of emory cloth at 90° to the first direction. Still others use a numbering technique in which they polish in one direction for 50 strokes, then rotate 90° and use a finer grade of polishing material for 50 strokes (*). Using these detailed and time-consuming methods of preparation, some degree of reproducibility has been achieved.

Clark, Strenge, and Westwater (24) have shown that after the most elaborate and detailed mechanical polishing techniques, pits and scratches remain on the surface. In addition, the authors demonstrated the diameters of active pits which were not removed by polishing were in the range of 0.0003-inch for their liquid surface combination. This was shown in Report I (1) to agree in magnitude with other results reported in the literature.

(*) Private communication with J. W. Westwater, University of Ill.

The vast majority of data present the nucleation sites as pits. Bankoff (25) has been able to show analytically that a pit presents a favored location for a nucleation site as opposed to a scratch or other surface discontinuity. This is not to imply ebullition will not occur from scratches but to state nucleation will occur from a pit in preference to a scratch. An excellent verification of Bankoff's theory is illustrated by a photograph in Ref. (24).

The mathematical model of a nucleation site used by many investigators has been discussed, Fig. 12, in Report I (1). In brief, this is a bubble located in an inverted conical pit. As in most mathematical models, this is an approximation to the actual shape of the nucleation site. Photographic investigations (24, 13) have verified the usefulness of this model.

Various attempts have been made to control the size and shape of the cavities. In addition to surface polishing, Bonilla, Grady, and Avery (26) presented data from highly polished surfaces in which scratches were scribed. In a similar study, Nishikawa (27) cut grooves of triangular cross section concentrically or crosswise on both smooth and rough surfaces. Griffith and Wallis (7) used a sharpened gramophone needle to give thirty-seven holes of uniform size and shape on a polished surface. In a comprehensive study, Berenson (20) provided data on the effect of lapping a surface. Westwater (28) summarizes the state of the art of surface preparation and states the need for data on surfaces chemically and electrolytically etched. The aim of the next phase of this study will be to obtain data for chemically etched Type 304 stainless steel.

b) Chemical Etching

The mechanism of corrosion will be discussed briefly. Since Type 304 stainless steel is the specimen material, the discussion will be limited to the theory of corrosion as applied to this material. The literature reveals numerous data on boiling heat transfer using Type 304 stainless steel as the surface material and this study will involve the same material. Type 304 stainless steel has the following properties:

TABLE II

Chemical Composition of 304 Stainless Steel

(Data As Specified by AISI)

C		P
.08 max		.045 max
Mn	Cr	S
2.00 Max	18 to 20.00	.030 Max
Si		Ni
1.00 Max		8 to 12.00

Physical Properties

Melting Point (°F)	Density (lb/m^3)	Specific Heat (Btu/lb °F)	Electrical Resistance /cm/cm^2	Thermal Conductivity Btu/hr/ft^2/ft/°F
2550	.29	32-212°F .12	72	212°F 9.4 932°F 12.4

Thermal Treatment	Hardening (°F)	2100-2300
	Initial forging (°F)	
	Annealing (°F)	Cools rapidly from 1850-2050
	Creep strength (1% flow in 10,000 hr at 1000°F	Hardenable by cold work only 17000 psi

Passive metals such as the stainless steels resist many corrosive media over long periods of time. However, if corrosion does eventually occur, rapid penetration takes place at several small areas. These are so-called "pits". They occur at random within or at the grain boundaries of the alloy. Several different forms of corrosion may occur with any metal. These forms are classified as fretting, galvanic, crevice, and pitting. Pitting is the prevalent form of corrosion experienced with the passive alloys and the passive metals such as aluminum, nickel, and chromium. The predominance of pitting corrosion in stainless steel may be advantageous to the boiling process.

The formation of pits begins by breakdown of passivity at favored (nuclei) on the metal surface. The breakdown is followed by formation of an electrolytic cell which consists of an anode of active metal and a large cathode of passive metal. Figure 18 depicts a typical electrolytic cell. The large potential difference characteristic of this "passive-active cell" (.5 to .6 volt for Type 304) accounts for considerable flow of current. The corrosion-resistant passive metal surrounding the anode and the activating property of the corrosion products within the pit along with the effect of gravity account for the tendency of corrosion to penetrate the metal rather than spread along the surface. The large potential of the cell accounts for a large effective cathode area, thereby drawing upon a considerable volume of depolarizer (dissolved oxygen or oxidizing salt) for maintenance of corrosion currents. Two heats of stainless steel of the same over-all analysis and in the same environment will show different tendencies toward pitting. On the other hand, the same alloy will pit profusely or not at all, depending upon enviromental conditions such

as temperature, pressure, water vapor, and oxygen content.

Pitting is most likely to occur in the presence of chloride ions combined with such depolarizers as oxygen or oxidizing salts. The oxidizing agent acts as a depolarizer for passive-active cells established by breakdown of passivity at a specific point or area. The chloride ion or other halogen ions can accomplish this breakdown. In solutions of chlorides, pitting occurs if the standard oxidation-reduction potential is less than -.15 volt. Table III shows various solutions and corresponding oxidation-reduction potentials.

TABLE III

Oxidation-Reduction Potential and Its Relation To Pitting For Several Solutions

(Data taken from Ref. 29)

Solution	Oxidation-Reduction Potential	Standard Potential	Presence of Pits After 24 Hr. Test
Hypochlorous Acid	$H^+ + HClO \rightarrow \frac{1}{2} Cl_2 + H_2O - e^-$	-1.63	+
Thallic Chloride	$Tl^{+++} + Cl^- \rightarrow TlCl - 2e^-$	-1.36	+
Mercuric Chloride	$2Hg^{++} \rightarrow Hg2^{++} + 2e^-$	-0.91	+
Ferric Chloride	$Fe^{+++} \rightarrow Fe^{++} - e^-$	- .77	+
Cupric Chloride	$Cu^{++} + Cl^- \rightarrow CuCl - e^-$	- .57	+
Stannic Chloride	$Sn^{+++} \rightarrow Sn^{++} - 2e^-$	- .15	-
Nickel Chloride	No lower valence Salt	0	-
Manganese Chloride	No lower valence Salt	0	-
Chromic Chloride	$Cr^{+++} \rightarrow Cr^{++} - e^-$	+ .41	-

If hydrogen peroxide is added to nickel chloride solutions, as in electroplating baths operating at about 60°C, the stainless steels pit severely. Accordingly, this indicates the oxidation-reduction potential is more negative than the -.15 volts. Pit nuclei have numerous sources. They occur through minor alloy components or impurities, or through heat treatment or mechanical work. Their exact nature is largely unknown. (29)

The use of many specimens in the boiling test dictates a corrosion media that will corrode the specimen quite rapidly. By far, the most effective agents are compounds containing elements of the halogen group. The use of sulphuric acid in non-aerated solutions generally results in a very slow corrosion rate. (30) Nitric acid, an oxidizing agent, in presence of a passive metal such as 304 stainless requires a very long time for appreciable pitting. Several organic acids, oxalic, formic, and lactic and a photographic solution containing thiosulfate, will be considered for this study. (31)

V. Data Collection

Considering the necessity of reproducible data the following sequences have been established for obtaining data. The specimens for both the surface and pressure effects studies will be mechanically polished using several grades of emory cloth. The final luster will be applied by using aluminum oxide or diamontine, whichever proves more practical to use. A modification of Gaertner and Westwater's (22) method of surface preparation will be followed at this stage.

This method consists of

1. 1300 cylic polishing strokes with 320 grit paper
2. 1500 cylic polishing strokes with 400 grit paper 90° to the first direction
3. 1200 cylic strokes with 600 grit paper in the original direction

Once the surface is properly prepared, the specimen will be placed in the boiler and subjected to a vacuum, as described in Chapter III of Report I (1). When the system has been out-gassed, the boiler will be filled with prepared water from the purification loop. At this time, current will be applied to the specimen and the bake-out or stabilization period will commence. When thermal equilibrium is reached the surface effects studies or transient studies can begin. These studies are described in the following sections A and B.

A) Surface Effects Procedure

The procedure for surface effects study data points will be followed upon reaching thermal-equilibrium. Suitable parameters will be varied for the initial tests with polished surfaces and a high speed motion picture record will be made of the phenomena associated with the parametric variation. As soon as sufficient data has been obtained the system pressure relief valve will open and the transient study will begin. The transient study as stated is described in section B. With the transient phase completed, a new sequence will be initiated using the same specimen. This method will be completed for three data runs on each specimen in the precorrosion stage. At this point, the specimen will be removed from the boiler and subjected to a corrosive electrolyte. There will be three different electrolytes with three specimens for each solution. Each specimen will be removed from the electrolyte after a specified time interval, cleaned, and placed in the boiler for three data runs, as described previously.

This method of data sampling will provide three curves of before-and-after corrosion information. From the three curves, the method of least squares may be applied to obtain a composite curve for the before-and-after state. The before curve can be compared to available data in order to ascertain if the technique provides acceptable data. The after curves can be compared to the before curves to determine the effect of corrosion on the heat-transfer coefficient. This will result in fifty-four runs.

The fifty-four runs along with photographic information should provide sufficient data to determine surface characterization. The correlation

equations discussed in Report I (1) will be compared by using data from this experiment. A new correlation equation will be formulated if an existing equation will not predict the results obtained in this experiment.

B) Transient Pressure Procedure

The procedure for the transient studies will commence after data collection for thermal-equilbrium conditions have been met. The system will be depressurized from saturation conditions at 100 psia. Prior to depressurization a steady-state pressure versus heat flux curve will be obtained. This curve will be compared with those of previous investigators (8), (9). Then the system will be depressurized from a high steady-state pressure using one of three orifice plates in the discharge line. The three orifice sizes are 1.0, 2.0, and 3.0 inches in diameter. High-speed photographs will be taken during the depressurization process and system pressure will be recorded.

VI. SUMMARY AND CONCLUSIONS

The literature reveals an increasing interest in transient parametric effects on boiling heat transfer. The steady state boiling phenomenon is not completely understood but transient phenomenon can be approached by considering the process under study to be a series of steady-state processes. This assumption will be limited by the uncertainity of present steady-state theory. However, this is the first logical step in an analysis of the parameter, pressure. The discussion of the pressure parameter in Chapter II revealed:

(1) Wall superheat increases at constant heat flux (8, 9, 10) as pressure is decreased. Figures 3 and 4 show this effect.

(2) The critical site radius, a function of wall superheat, increases with an increase in pressure.

(3) The active site density increases with an increase in pressure as shown in Fig. 7.

(4) The agitation of the fluid due to bubble motion is reduced as pressure increases. As seen from Figs. 9 and 10, the frequency and departure diameter is reduced with an increase in pressure (13).

(5) The thermal boundary layer thickness of superheated liquid above a heater surface decreases with a pressure increase.

Review of the surface effects on boiling heat transfer indicates the necessity for systematic investigation before the phenomenon is fully

understood. Some of the factors involved in a careful study include, a method of accurately measuring the surface topography, a standard method of surface preparation, and an accurate and efficient method of data compiling. In particular Chapter III revealed:

(1) The Profilometer is not a satisfactory instrument for surface characterization.

(2) The Linear Proficorder, an optical comparator, and the replica technique provide possible methods of surface characterization. At this time, the Linear Proficorder appears to be the most promising method.

(3) A modification of Gaertner and Westwater's method of mechanical polishing will be used in the preliminary stages of specimen preparation.

(4) A solution using the chloride ion to destroy passivity will pit the surface of 304 stainless steel. This method of corrosion will be employed in the corrosion phase of study.

References Cited

1. G. E. Tanger, G. H. Nix, and D. L. Davis, Preliminary Investigation of Surface Roughness Influence on Multiphase Heat Transfer, Report I, Contract NAS8-11234, Auburn Research Foundation, September 1964.

2. S. W. Gouse, Jr., "An Index to the Two-Phase Gas-Liquid Flow Literature, Part I," MIT Engineering Projects Laboratory Report DSR 8734-1, Mechanical Engineering Department, May 1963.

3. R. R. Kepple and T. V. Tung, "Two-Phase (Gas-Liquid) Systems: Heat Transfer and Hydraulics," ANL 6734, Argonne National Laboratory, 1964.

4. J. R. Howell and K. J. Bell, "An Experimental Investigation of the Effect of Pressure Transients on Pool Boiling Burnout," AIChE Symposium Series, Vol. 59, No. 41, 1963, pp. 88-95.

5. M. S. Plesset and D. Y. Hsieh, "Theory of Gas Bubble Dynamics in Oscillating Pressure Fields," Report 85-16, Engineering Division California Institute of Technology, August 1960.

6. D. A. DiCicco and R. J. Schoenhals, "Heat Transfer in Film Boiling with Pulsating Pressures," Journal of Heat Transfer, ASME Transactions, Series C, Vol. 86, No. 3, August 1964, pp. 457-461.

7. P. Griffith and J. D. Wallis, "The Role of Surface Conditions in Nucleate Boiling," AIChE Symposium Series, Vol. 56, No. 30, 1960, pp. 49-63.

8. E. A. Farber and R. L. Scorah, "Heat Transfer to Water Boiling Under Pressure," ASME Transactions, Vol. 50, 1948, pp. 369-384.

9. M. T. Cichelli and C. F. Bonilla, "Heat Transfer to Liquids Under Pressure," AIChE Transactions, Vol. 41, 1945, pp. 755-787.

10. W. M. Rohsenow, "Heat Transfer with Boiling," chapter in Modern Developments in Heat Transfer, Edited by W. Ibele, Academic Press New York, 1963.

11. I. A. Raben, et al., "A Study of Nucleate Pool Boiling of Water at Low Pressure," AIChE Preprint No. 28, presented at the Sixth National Heat-Transfer Conference, Boston, Massachusetts, August 11-14, 1963.

12. C. Corty and A. S. Foust, "Surface Variables in Nucleate Boiling," Chemical Engineering Progress Symposium Series, Vol. 51, No. 17, 1955, pp. 1-12.

13. S. S. Kutateladze, "Heat Transfer in Condensation and Boiling," AEC-tr-3770, United States Atomic Energy Commission, Technical Information Service, (1952).

14. S. G. Bankoff, "Prediction of Surface Temperatures at Incipient Boiling," AIChE Symposium Series, Vol. 55, No. 29, 1959.

15. M. Jakob, Heat Transfer, Vol. I, John Wiley & Sons, Inc., New York, 1949, pp. 631-642.

16. W. Fritz and W. Ende, "Verdampfungsvorgangnach Kinematographischen Aufnahmen an Dampfblasen," Phys. Zeitsh, Vol. 37, 1936, pp. 401.

17. N. Zuber, "Hydrodynamic Aspects of Boiling Heat Transfer," AECU-4439, USAEC Technical Information Services, (June 1959).

18. C. J. Rallis and H. H. Jawurek, "Latent Heat Transport in Saturated Nucleate Boiling," International Journal of Heat and Mass Transfer, Vol. 7, No. 10, 1964, pp. 1051-1067.

19. J. W. Westwater, "Nucleate Boiling," Petroleum Management, Vol. 33, (August 1961) pp. 186-189.

20. P. J. Berenson, "Experiments on Pool Boiling Heat Transfer," International Journal of Heat and Mass Transfer, Vol. 5, 1962, pp. 985-999.

21. F. G. Hammitt, et. al., "Cavitation Damage Test with Water in a Cavitating Venturi," Technical Report, Office of Research Administration, University of Michigan, NASA grant No. NSG-39-48.

22. R. F. Gaertner and J. W. Westwater, "Population of Active Sites in Nucleate Boiling Heat Transfer," Chemical Engineering Progress Symposium Series, Vol. 56, No. 30, 1960, pp. 39-48.

23. H. W. Maynor, C. J. McHargue, and O. F. Edwards, "Comparison of Electron and Optical Photomicrographs of a Copper-Beryllium Alloy" Transactions of the Kentucky Academy of Science, Vol. 13, No. 4, August, 1952.

24. H. B. Clark, P. S. Strenge, and J. W. Westwater, "Active Sites of Nucleate Boiling," Chemical Engineering Progress Symposium Series, Vol. 55, No. 29, 1959, pp. 103-110.

25. S. G. Bankoff, "Ebullition from Solid Surfaces in the Absence of Pre-Existing Gaseous Phase," Proceedings Heat Transfer and Fluid Mechanics Institute, 1956.

26. C. F. Bonilla, J. J. Grady, and G. W. Auery, "Pool Boiling Heat Transfer from Scored Surfaces," AICHE Preprint 32, Sixth National Heat Transfer Conference, August 1963.

27. K. Nishikawa, "Nucleate Boiling Heat Transfer of Water on the Horizontal Roughened Surface," Memoirs of the Faculty of Engineering, Kyushu University, Vol. 17, No. 2, 1958, pp. 85-103.

28. J. W. Westwater, "Things We Don't Know About Boiling Heat Transfer," Pergamon Press, New York, 1963.

29. H. H. Uhlig, "Pitting in Stainless Steels and Other Passive Metals," Corrosion Handbook, John Wiley and Sons, New York, New York, 1948, pp. 165-173.

30. W. O. Binder, "Corrosion Resistance of Stainless Steels and High Nickel Alloys," Corrosion of Metals, American Society for Metals, Cleveland, Ohio, 1946, pp. 51-99.

31. H. H. Uhlig, Corrosion and Corrosion Control, John Wiley and Sons, New York, New York, 1964, pp. 259.

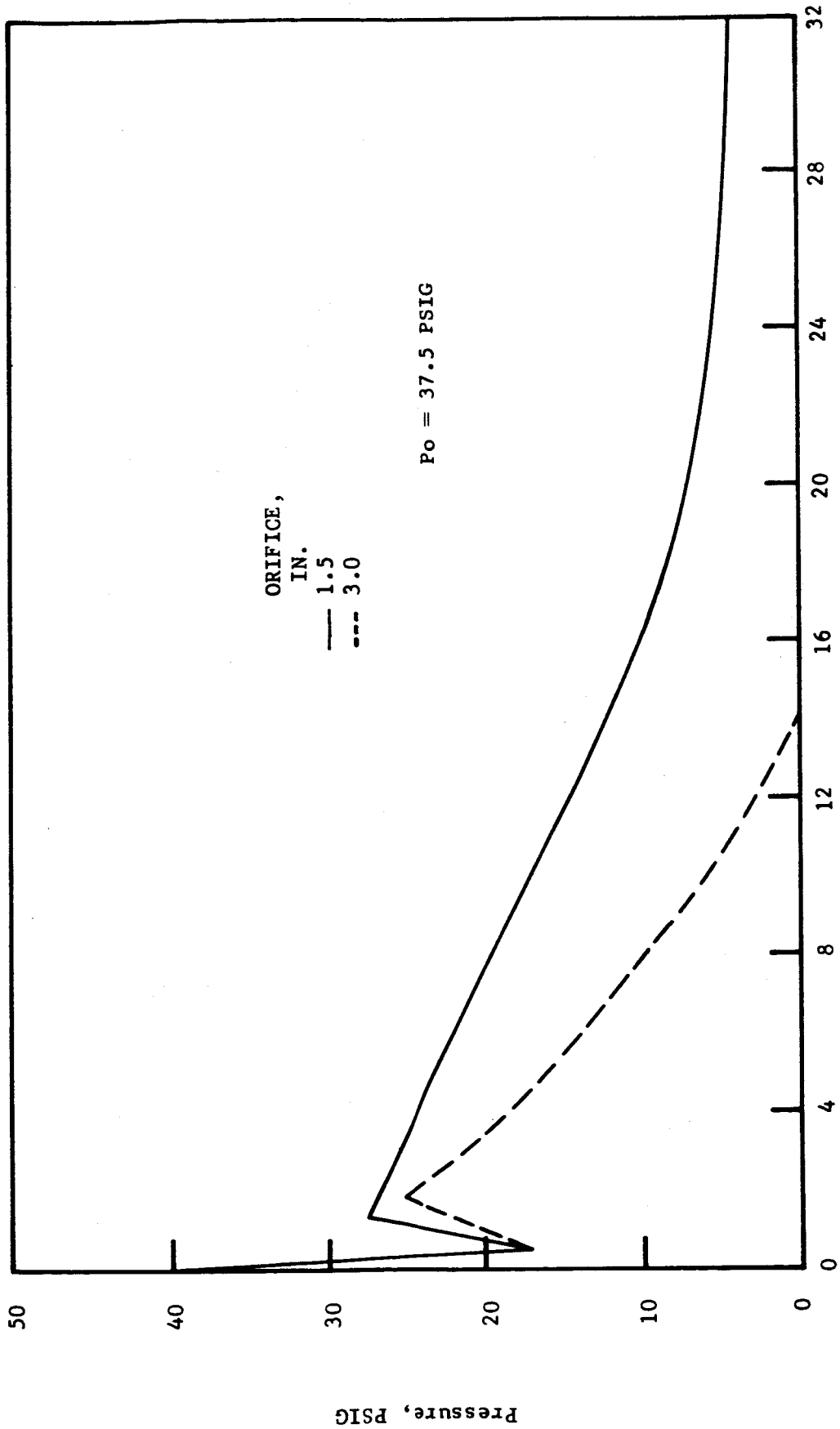

Fig. 1 Pressure Decay Curve (Fig. 3, ref. 4)

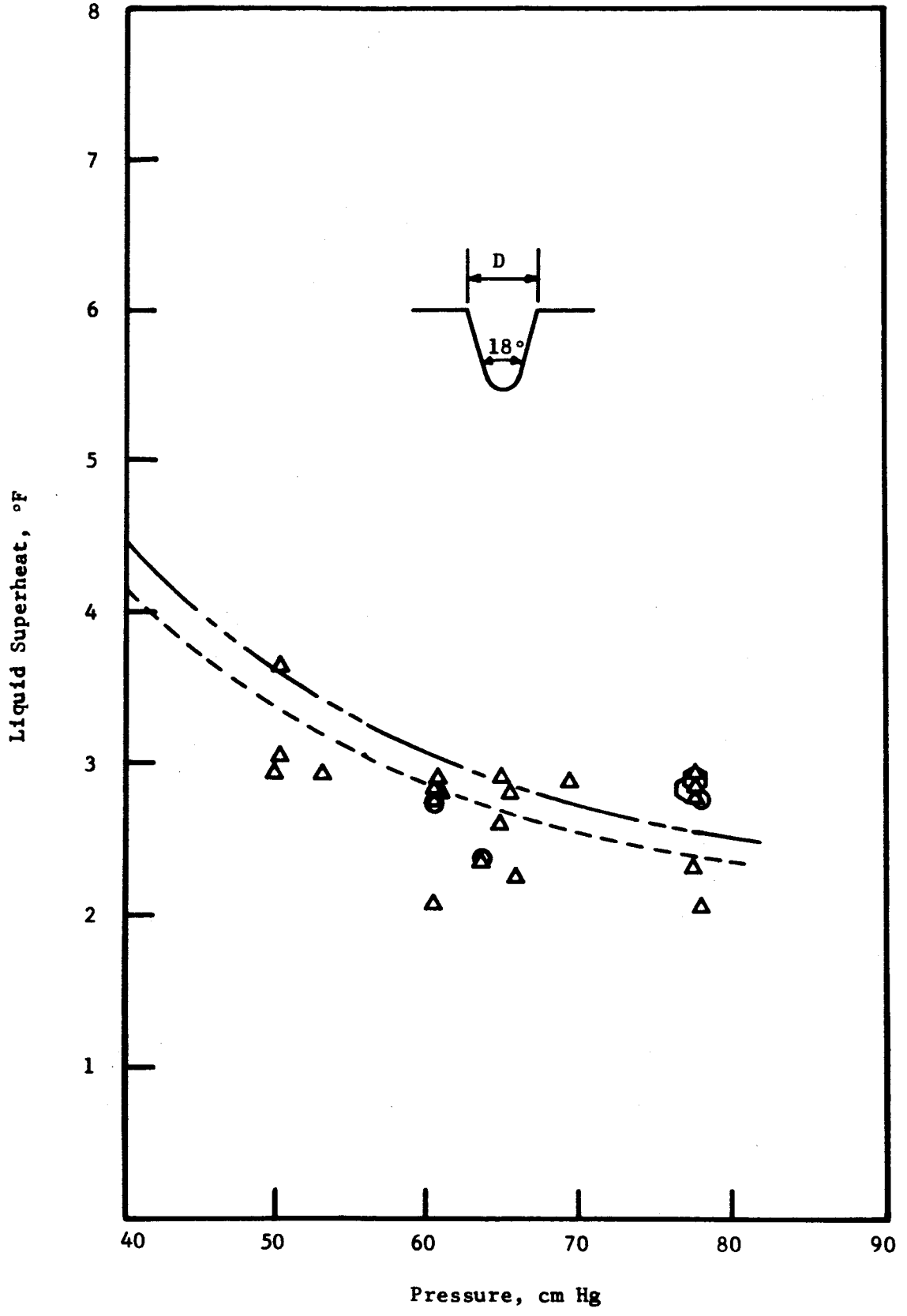

Fig. 2 Superheat Versus Pressure for Cavity of Diameter, D =0.0018 in. (data from Fig. 7, ref. 7)

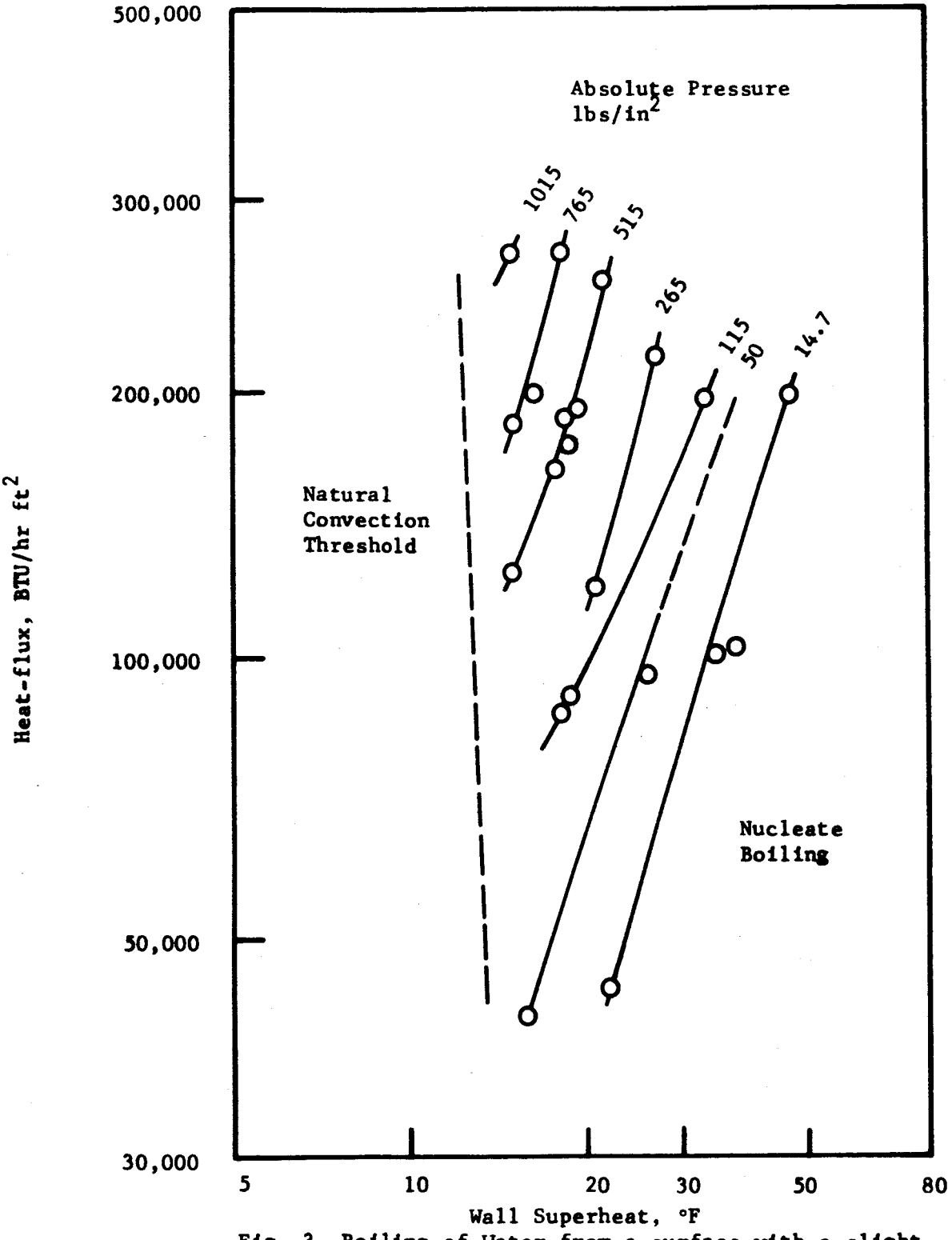

Fig. 3 Boiling of Water from a surface with a slight Scale Deposit (Fig. 10, ref. 9).

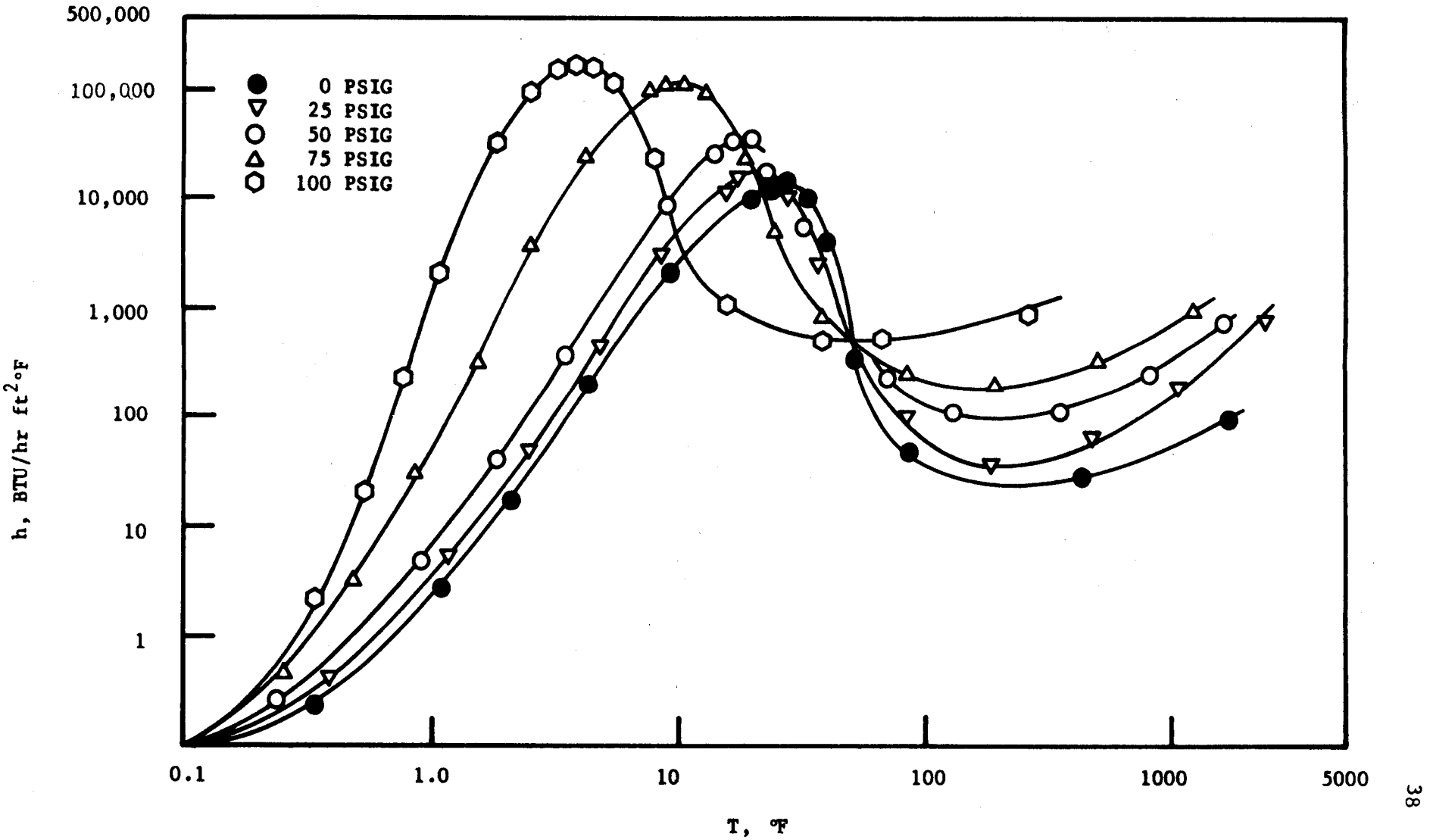

Fig. 4 Boiling Curves for Chromel A and Water
(Fig. 10, ref. 8)

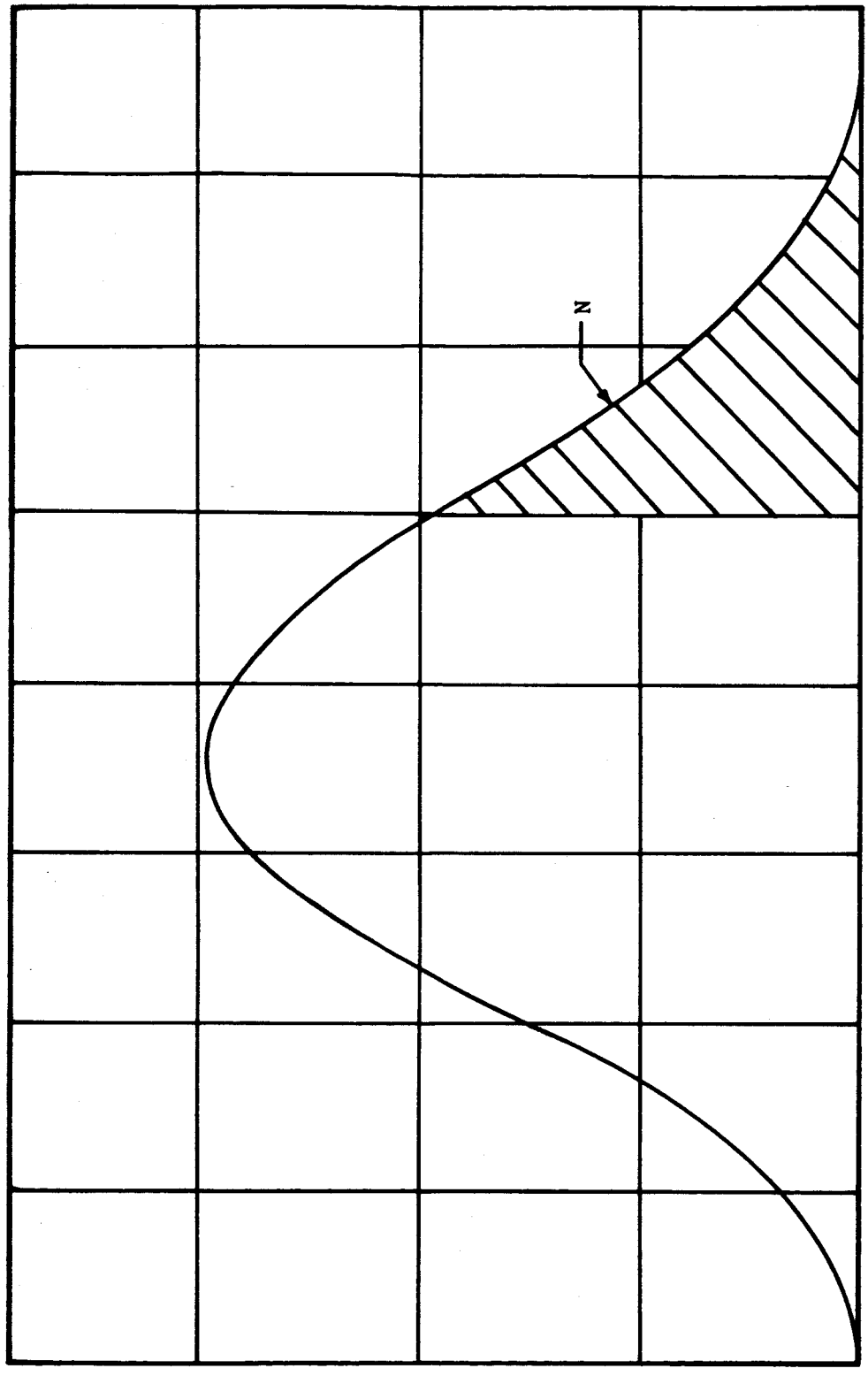

Fig. 5 Sketch of Cavity Size Distribution Function
(Fig. 27, ref. 10)

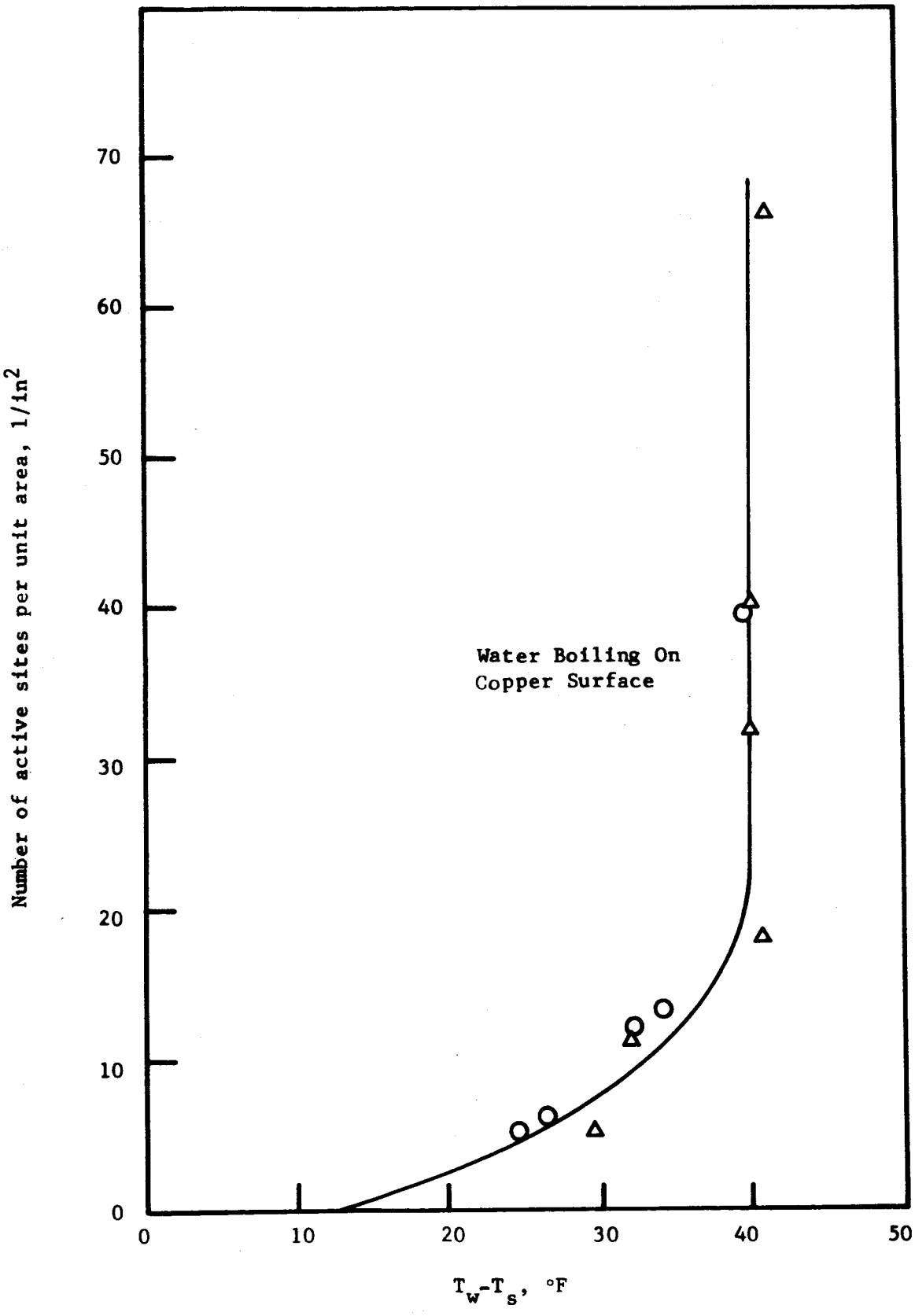

Fig. 6 Number of Active Sites per Unit Area Versus Wall Superheat (data from Fig. 9, ref. 7)

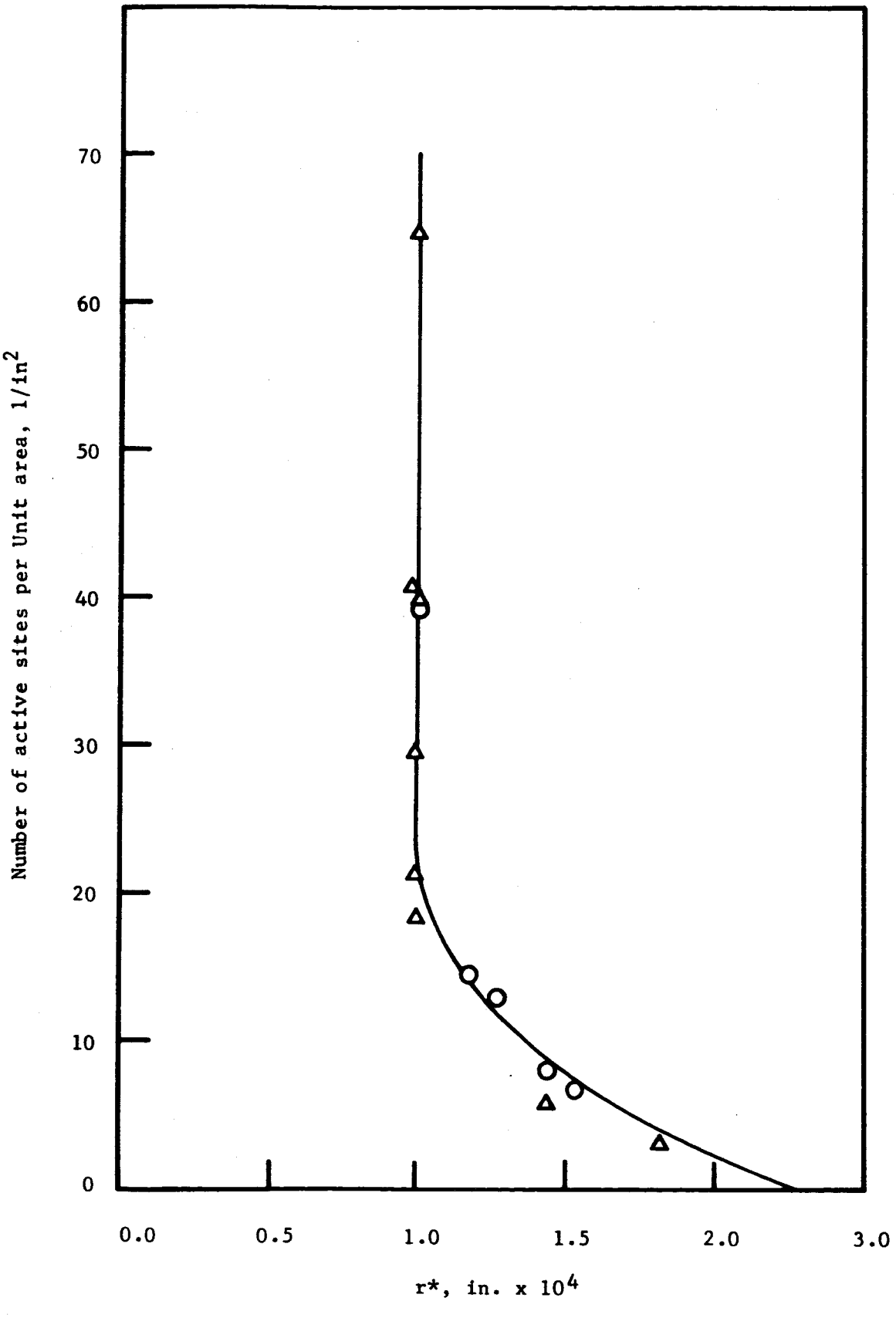

Fig. 7 Number of Active Sites per Unit Area Versus Critical Cavity Radius (data from Fig. 10, ref. 7)

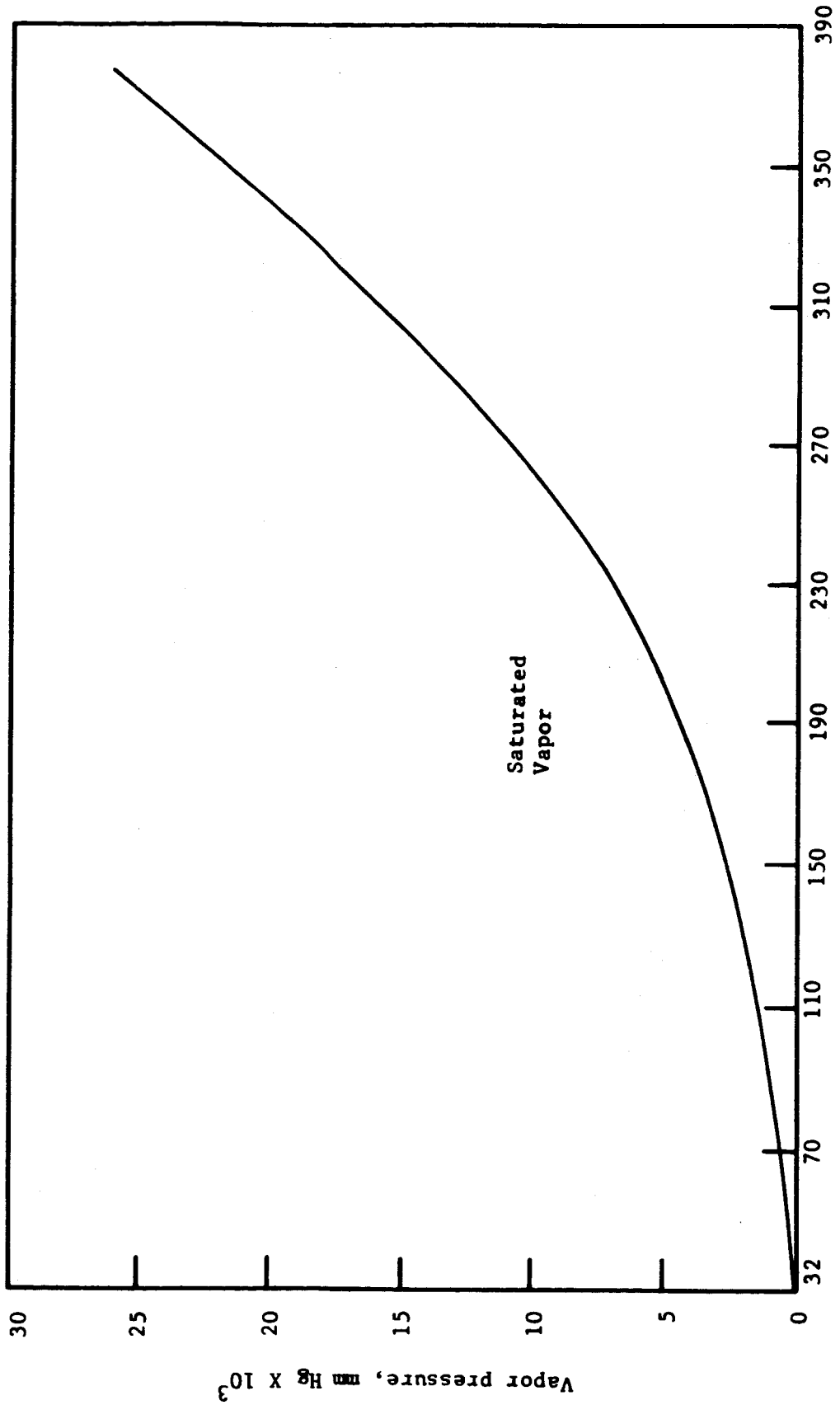

Fig. 8 Vapor Pressure Versus Temperature
For Saturated Water
(Fig. 13, ref. 10)

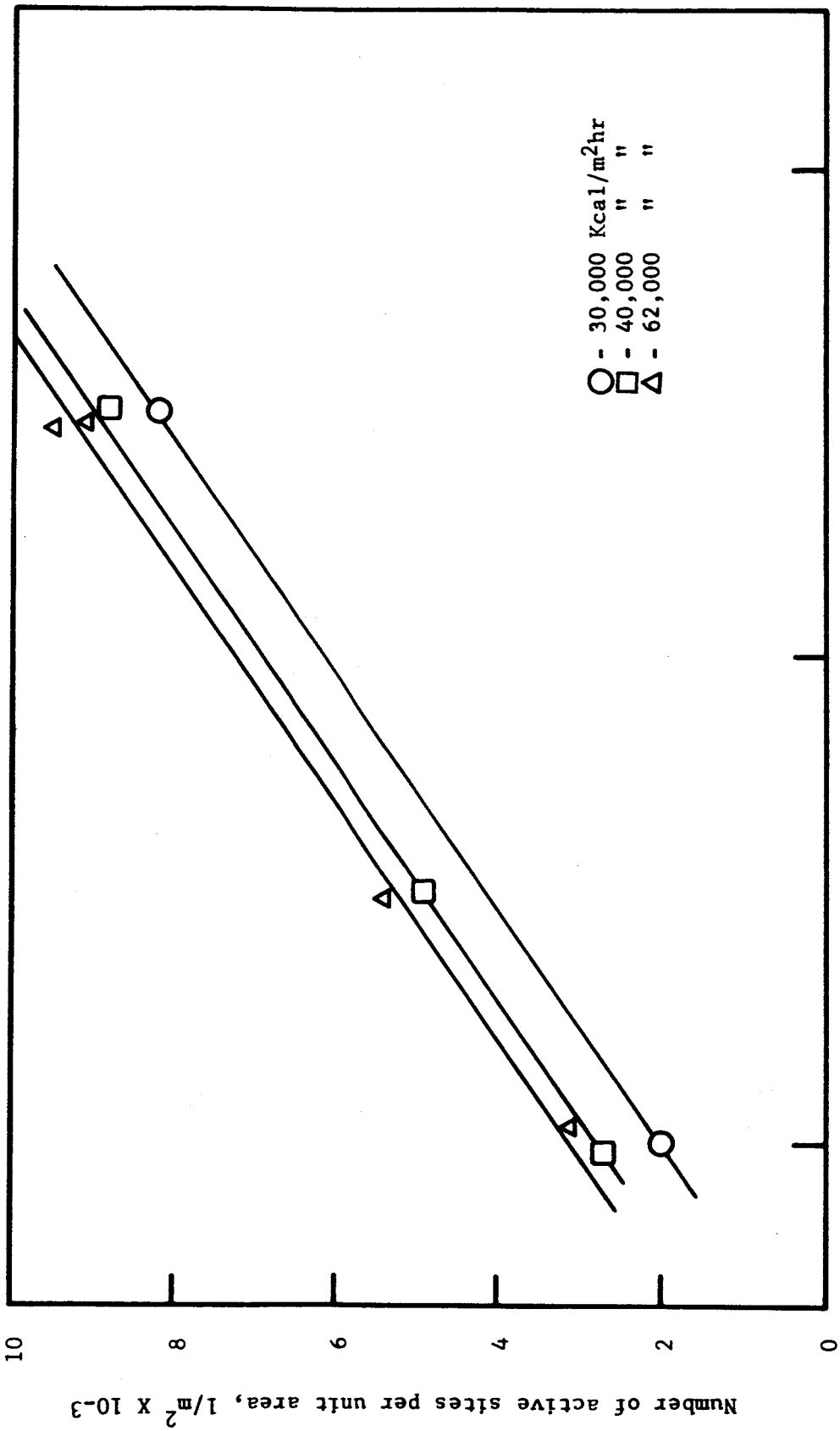

Fig. 9 Number of Active Sites per unit area versus pressure for water boiling on Flat Plate (data from Fig. 57, ref. 13)

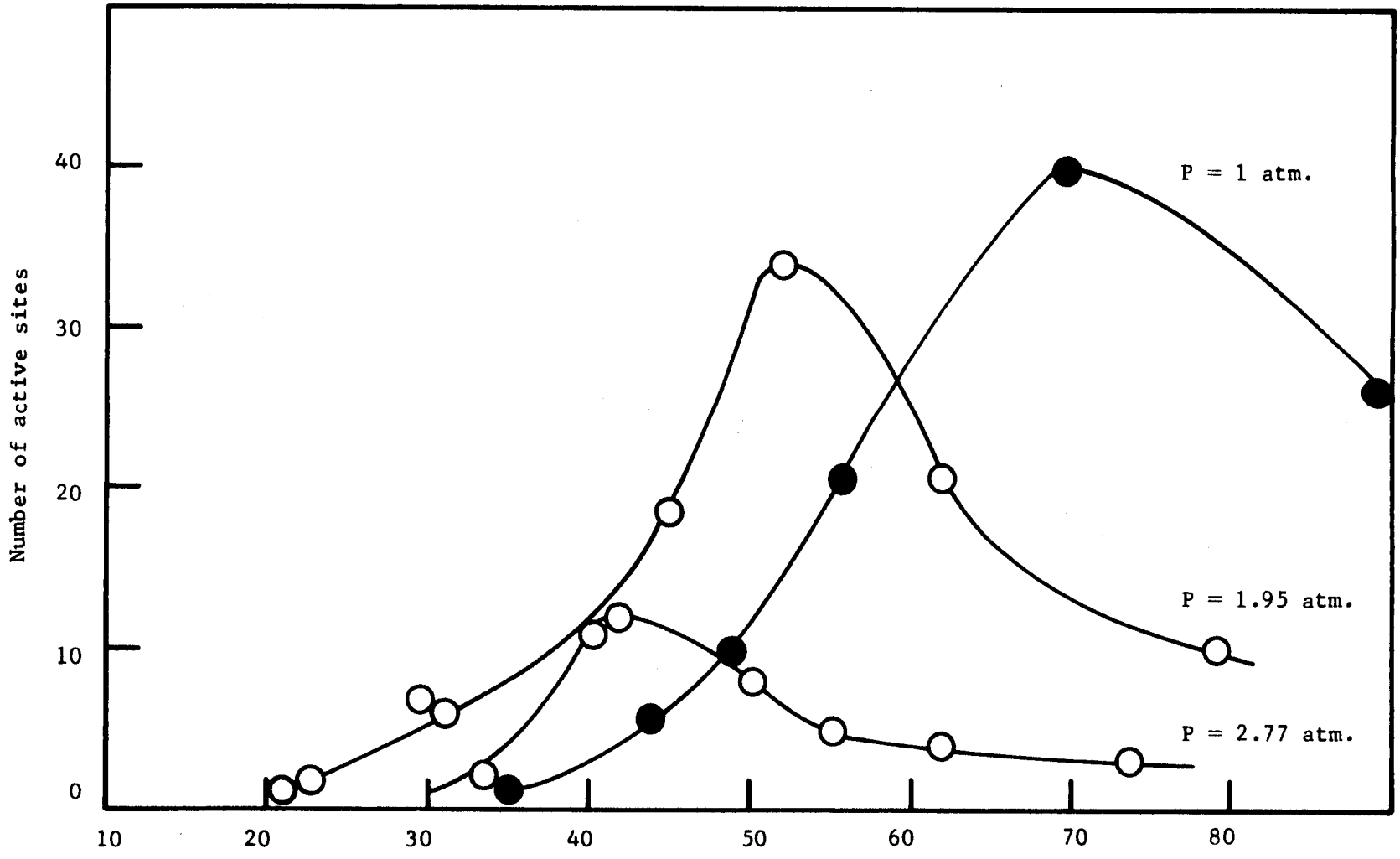

Fig. 10 Distribution of Active Sites Versus Rate of Bubble Formation (data from Fig. 40, ref. 13)

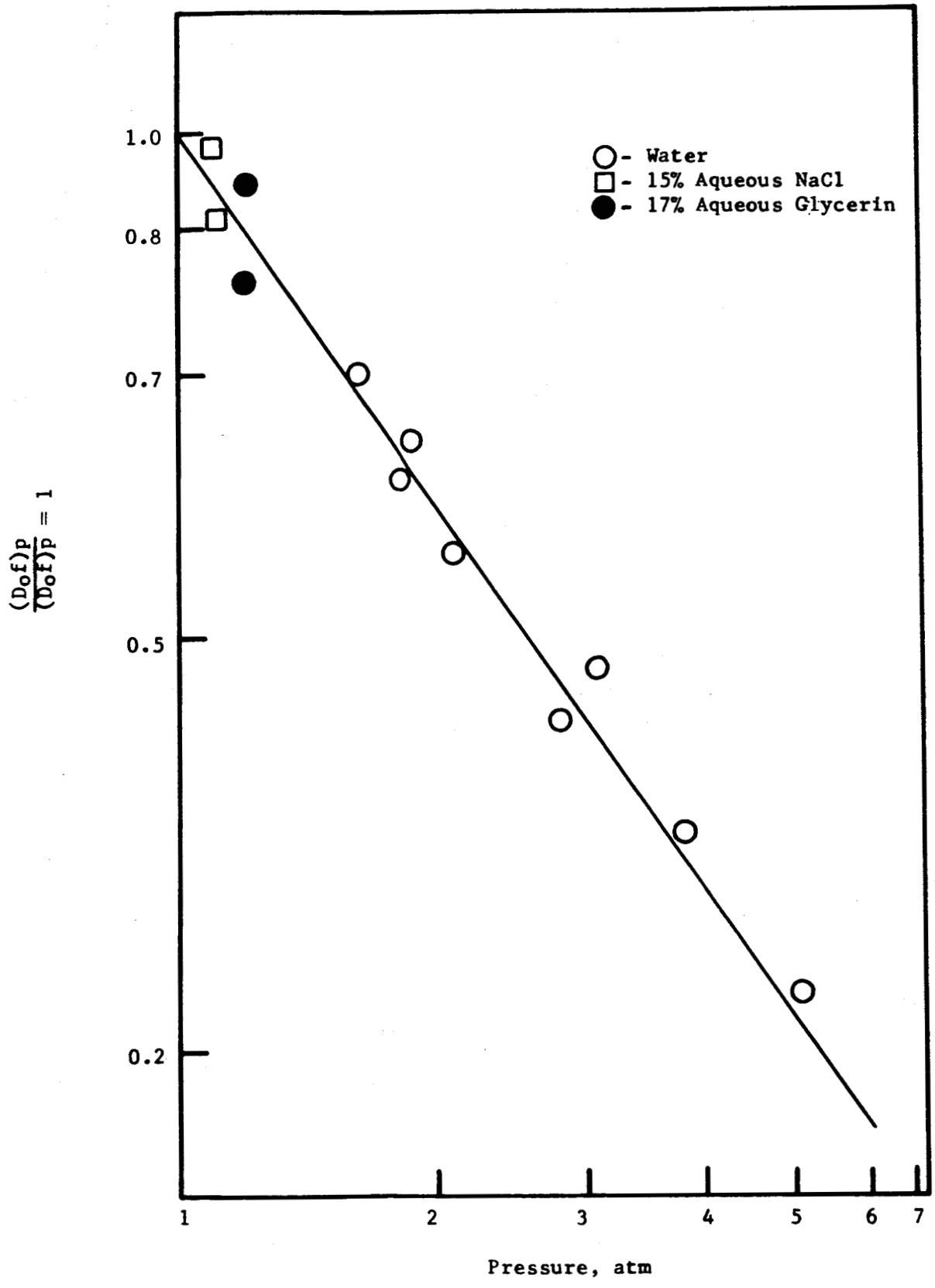

Fig. 11 Relative Change in the Term $D_o f$ with Pressure (Fig. 41, ref. 13)

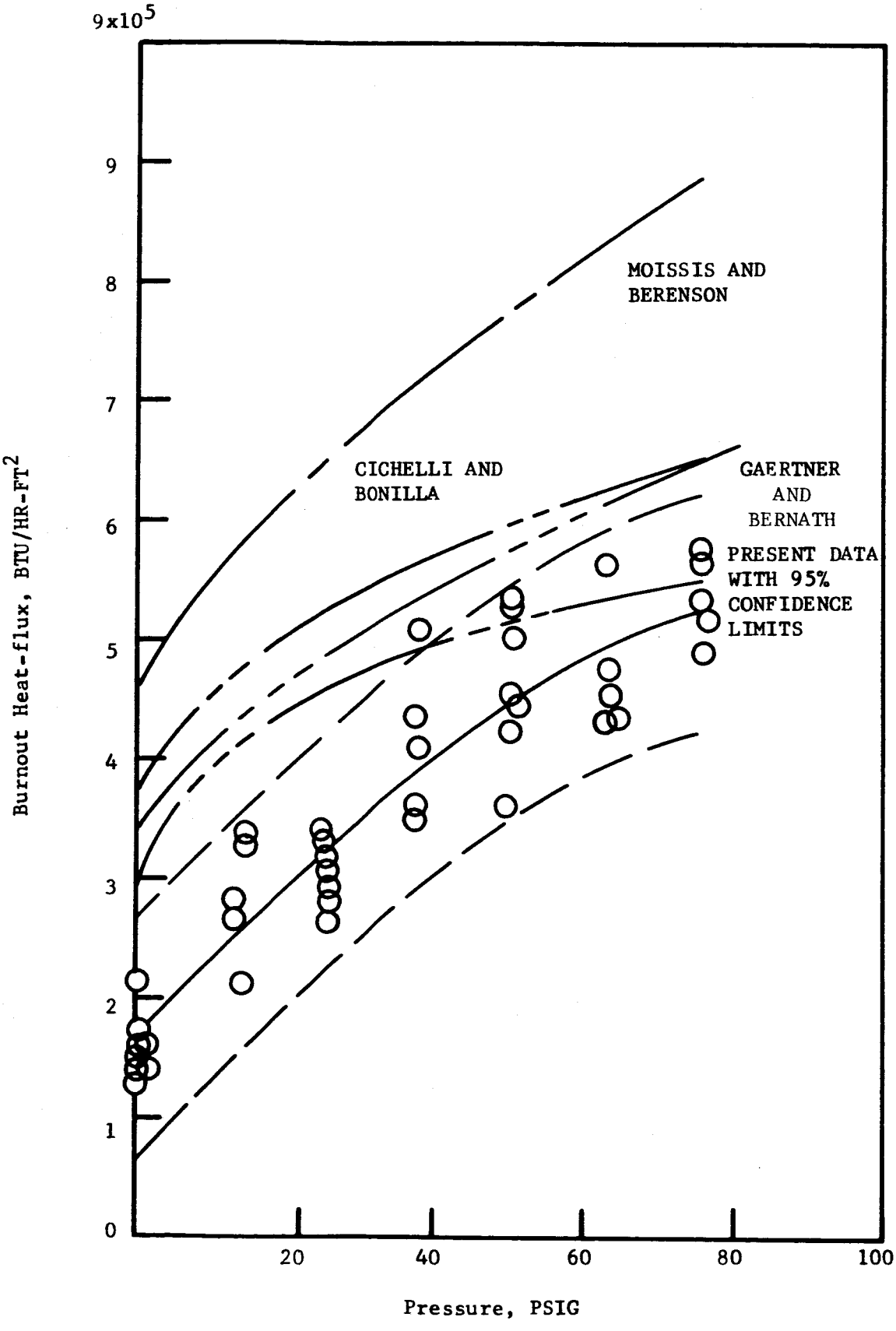

Fig. 12 Steady-state Burnout Heat-flux Versus Pressure (Fig. 2, ref. 4)

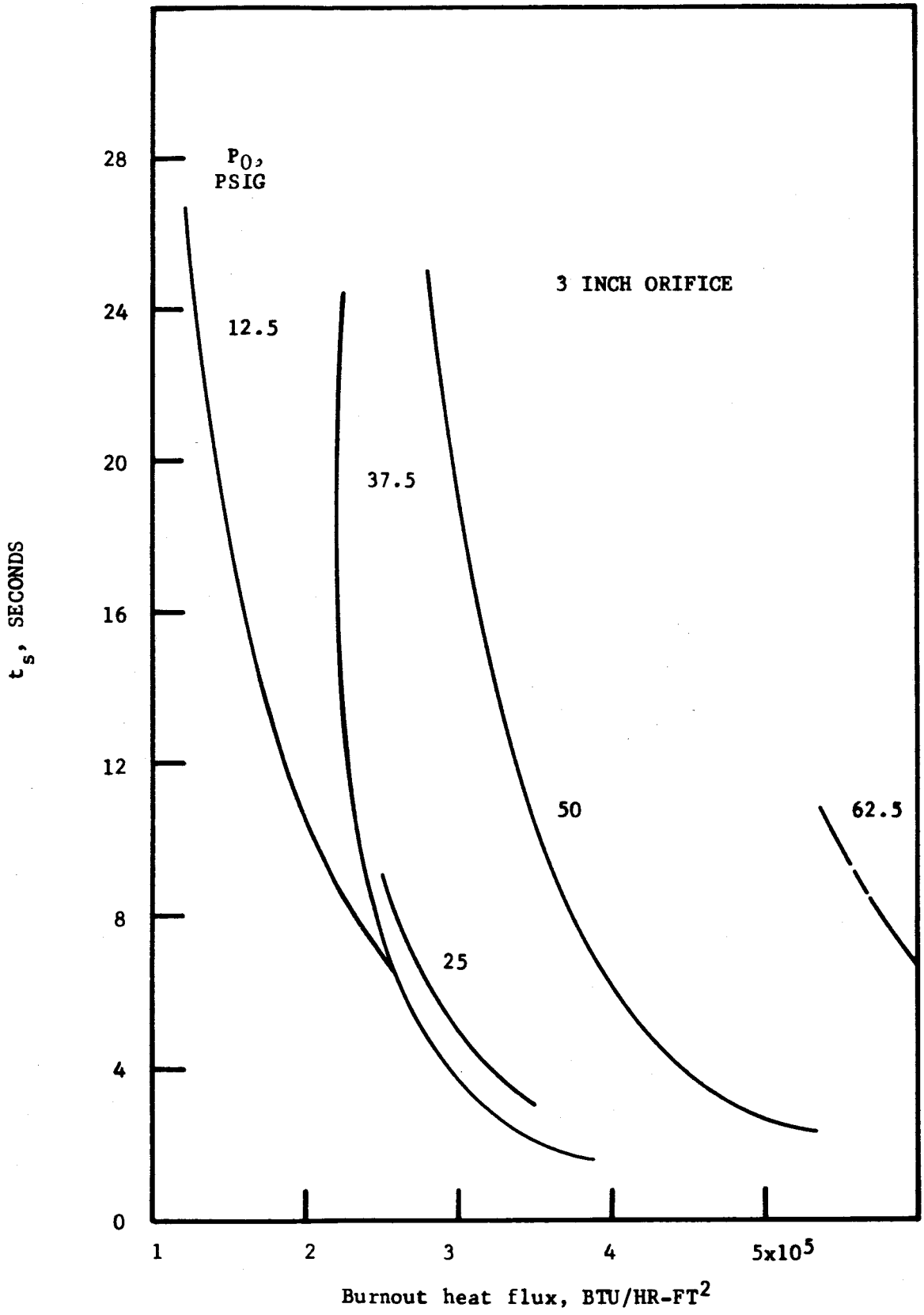

Fig. 13 Transient Burnout Curves.

(Fig. 5a, ref. 4)

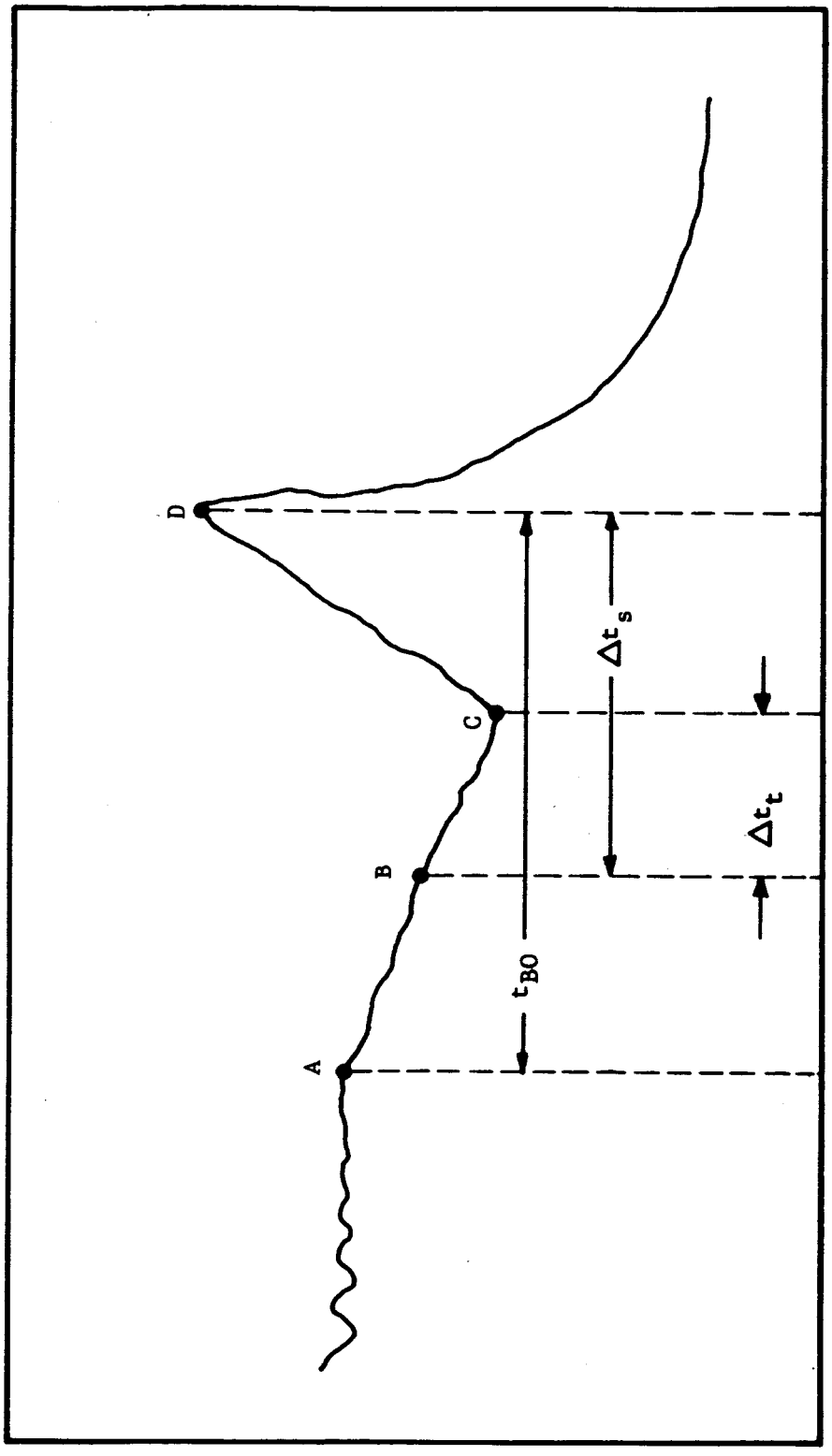

Fig. 14 Definition of Time Nomenclature for Transient Burnout Study (Fig. 4a, ref. 4)

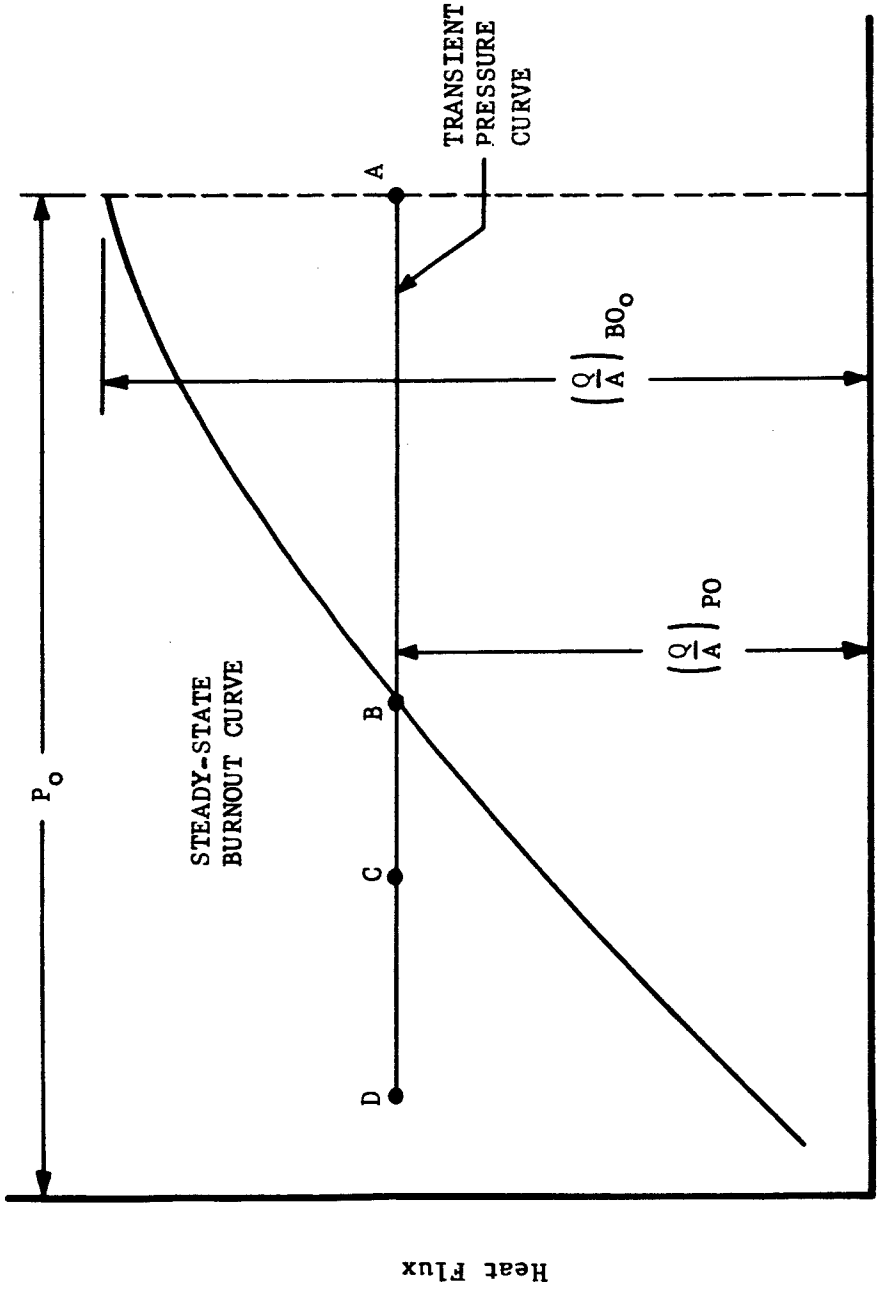

Fig. 15 Definition of Nomenclature for Transient Pressure Run (Fig. 4b, ref. 4)

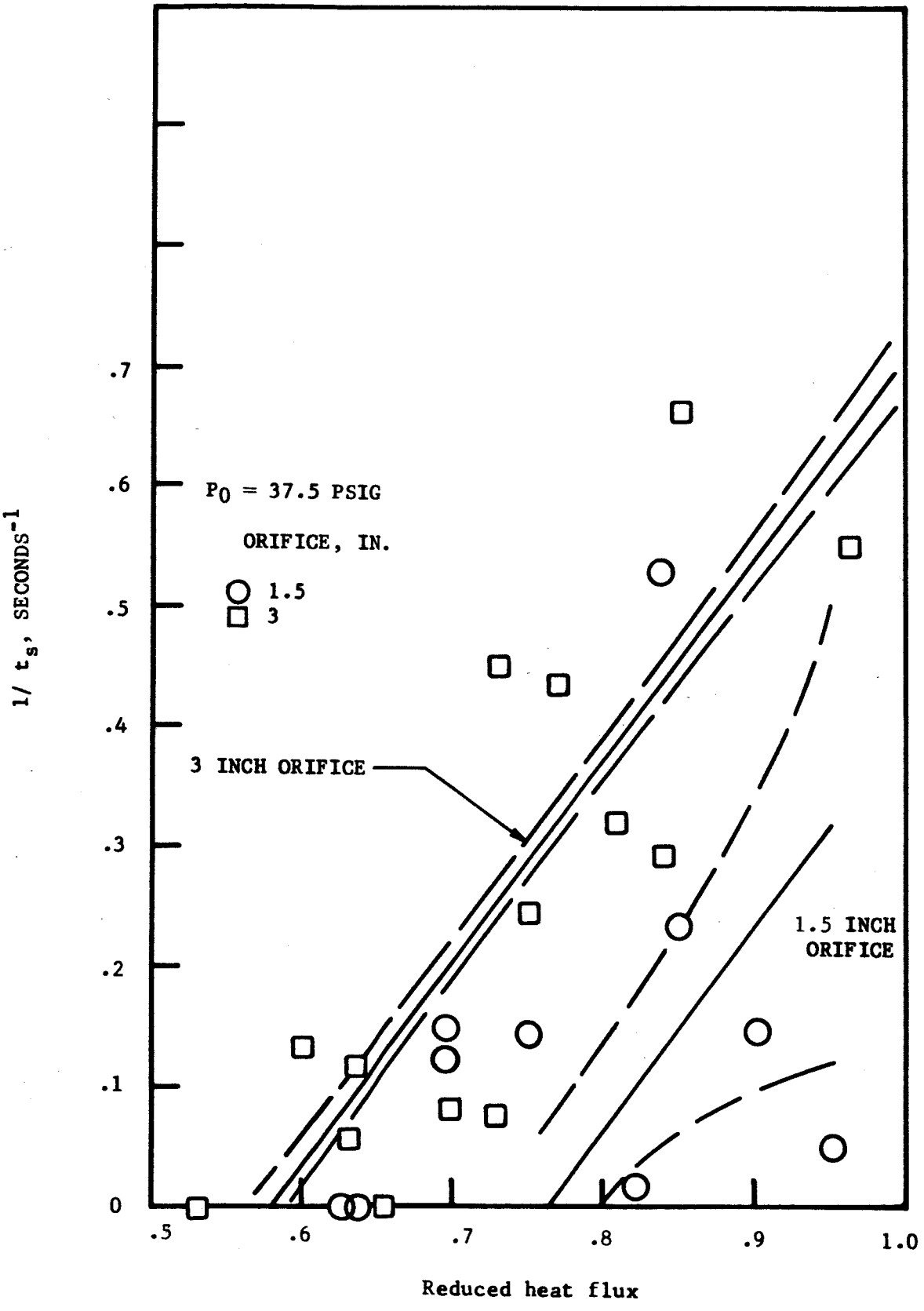

Fig. 16 Comparison of Pressure Release Rates (Fig. 6a, ref. 4)

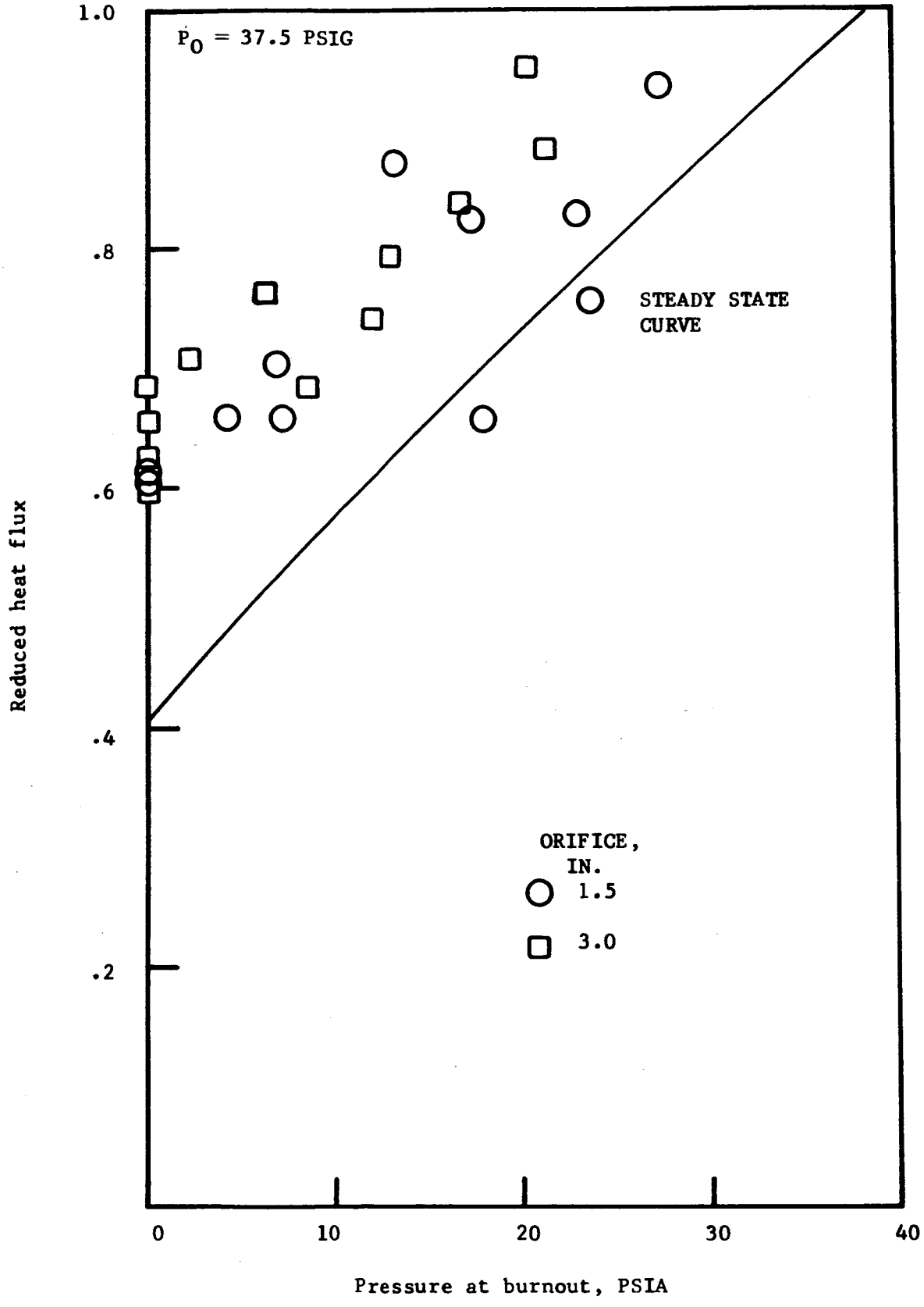

Fig. 17 Reduced heat flux versus Burnout Pressure (Fig. 6b, ref. 4)

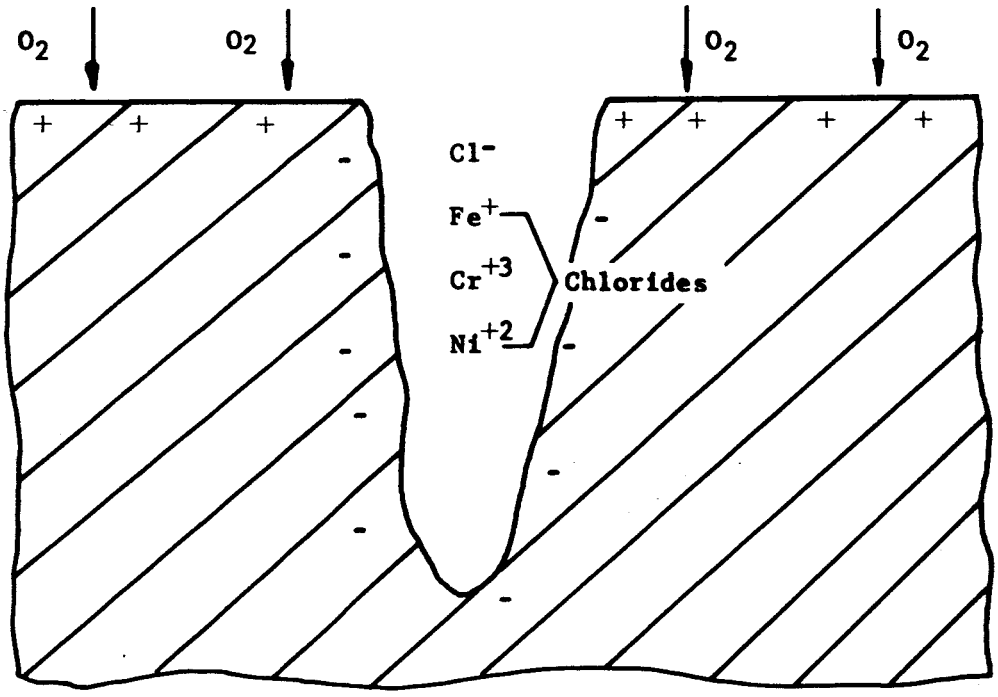

Fig. 18 Typical Electrolytic Cell formed in the pitting process of stainless steel.